# ÚJSZÜLÖTT-KORBAN RÖNTGEN SUGÁRRAL KÁROSÍTOTT PATKÁNY HIPPOKAMPUSZ VIZSGÁLATA MORFOLÓGIAI, ELEKTROFIZIOLÓGIAI ÉS MAGATARTÁS FIZIOLÓGIAI ELJÁRÁSOKKAL

EGYETEMI DOKTORI (PH.D.) ÉRTEKEZÉS


DR CZÉH BOLDIZSÁR

PÉCSI ORVOSTUDOMÁNYI EGYETEM

FARMAKOLÓGIAI ÉS FARMAKOTERÁPIAI INTÉZET


Témavezetô:

Dr, Ph.D. Seress László egyetemi docens

Központi Elektromikroszkópos Laboratórium

Programvezetô: Dr, Ph.D. Lénárd László egyetemi tanár

PÉCSI ORVOSTUDOMÁNYI EGYETEM

ÉLETTANI INTÉZET


PÉCS, 1998

# KÖSZÖNETNYÍLVÁNÍTÁS

Elöljáróban szeretnék köszönetet mondani mindazoknak, akik nélkül az itt bemutatásra kerülô kutatási eredmények nem jöhettek volna létre.

Köszönettel tartozom témavezetômnek dr Seress Lászlónak, kinek széleslátókörű irányítása segített e szerteágazó tanulmány létrehozásában és akinek laboratóriumában a szövettani technikákat elsajátítottam.

Köszönöm dr Czéh Gábor segítségét, e munka elektrofiziológiai részeinek megalkotásában.

Hálával tartozom dr Jan Buresnek, kinek útmutatásával, a Cseh Tudományos Akadémia (Prága) magatartás tudományi laboratóriumában a téri tájékozódási kisérleteket elvégeztük.

Köszönöm dr Czurkó András közremüködését, akivel az 5. fejezetben bemutatott kisérleteket közösen végeztük. Köszönöm Paleszter Mária aszisztensnô odaadó segítségét a szövettani munkákban.

Köszönettel tartozom továbbá az POTE Élettani Intézet munkatársainak és igazgatójának, dr Lénárd Lászlónak, az Idegtudományok Ph.D. Program vezetôjének, hogy intézetében kutathattam. Végül köszönöm dr Szolcsányi Jánosnak, a Gyógyszertani Intézet igazgatójának a hozzájárulását, intézete elektrofiziológiai laboratóriumának használatához.

Pécs, 1998 Szeptember 30.

# Effects of Neonatal X-Ray Irradiation on the Rat Hippocampus: Behavioral, Electrophysiological and Morphological Consequences of Partial Degranulation

**Dissertation**

submitted for the degree of

**Doctor of Philosophy**

by Boldizsár Czéh M.D.

Pécs, 1998.

## TABLE OF CONTENTS

# Chapter 1.

# GENERAL INTRODUCTION

The hippocampal formation of the mammalian brain has attracted the attention of neuroanatomists, physiologists and psychologists throughout this century. „Hippocampus" means „seahorse", so named because of its gross anatomical resemblance to a sea creature. The hippocampus was named in 1587 by the medieval anatomist Arantius (Rosene and Van Hoesen, 1987).

The hippocampus has been the focus of extensive anatomical investigation since the classic Golgi examinations carried out by Ramon y Cajal (1893), Lorente de No (1934), and Blackstad (1956) who focused on the basic structure of hippocampal organization. Current interest shifted from the gross anatomy of the hippocampus to the function attributed to this structure in behavior, and especially in learning and memory. The hippocampus has been implicated in spatial orientation (O'Keefe and Nadel, 1978; Morris, 1981; Morris et al., 1982; Nadel, 1991; Jarrard, 1993), emotions (Papez, 1937), motivation (Jarrard, 1973), and generalized information processing (Olton et al., 1979; Squire, 1987; Cohen and Eichenbaum, 1991). Despite this diversity of functions, the hippocampus has primarily been referred to as a mediator of learning and memory. Scoville and Milner (1957) proposed a positive correlation between the extent of hippocampal cellular loss and the degree of memory impairment when they described the case of H.M. H.M. suffered moderate retrograde amnesia and severe anterograde amnesia after complete, bilateral, surgical removal of the entire hippocampus. Bliss and Lomo (1973) reported that tetanic stimulation of the perforant pathway produced a long lasting, enhanced effect at the cellular level via an increase in synaptic efficacy. This "long term potentiation" effect within the hippocampus offered additional support for its involvement in memory formation. Subsequent spatial orientation studies (O'Keefe and Dostrovsky, 1971; O'Keefe, 1976; Wilson

and McNaughton, 1993) have shown that specific cells within the hippocampus are selectively active when an animal is placed in a particular location within its environment.

The hippocampus is one of the primary neural structures damaged during ischemia (Schmidt-Kastner and Freund, 1991), stroke (Pulsinelli et al., 1982), and Alzheimer's disease (Hyman et al., 1982). Specifically, the CA1 region of the hippocampus is the most vulnerable to the effects of stroke-induced ischemia (Volpe et al., 1992; Wood et al., 1993) inducing permanent memory deficits (Caronna, 1979; Volpe and Hirst, 1983; Cummings et al., 1984). Consistent with these clinical accounts, rats display memory dysfunctions when lesions are placed at various sites within the hippocampal formation. This memory loss is not a global amnesia, rather it is specific to spatial learning and memory tasks (Morris et al., 1982; Sutherland et al., 1982; Sutherland et al., 1983; Zola-Morgan et al., 1986). Therefore, a systematic evaluation of the relationship between specific hippocampal damage and behavioral impairment should be clinically relevant.

There are many neuro- and psychopathological conditions with presumed early developmental origin, but little is known about when, where, how, and what kind of events trigger abnormal development that leads to malformations in closely related anatomical structures and consequent behavioral disorders in adulthood.

Purpose of our experiments of basic research have been to describe functional and morphological consequences of the removal of a postnatally forming part of the hippocampus (granule cells) using a noninvasive method. In our model, a massive experimentally controlled destruction of the precursors of granule cells is the triggering event in the modified-development of the hippocampus, which causes electrophysiological and morphological changes of closely related anatomical structures and alter the behavior (spatial learning) of the adult rat.

**The animal model: the neonatally irradiated rat.**

Within the rodent brain, the granule cells of the hippocampal dentate gyrus represent one of the few neuronal populations which go through postnatal neurogenesis (Altman and Bayer, 1965; Bayer, 1980; Stanfield and Cowan, 1988). Neurogenesis of granule cells begins on embryonic day 17 in the rat (Bayer, 1980), but only 20% of these cells is present at the time of birth (Altman and Das, 1965; Bayer and Altman, 1975). Although the number seen in adult rats is reached late in the third postnatal week, neurogenesis continues throughout life (Altman and Bayer, 1965; Bayer, 1980; Crespo et al., 1986).

Since multiplying cells, unlike postmitotic and matured neurons, are extremely radiosensitive (Altman et al., 1969), X-ray irradiation selectively eliminates postnatally forming granule cells of the dentate gyrus (Bayer et al., 1973) and leaves their target neurons (CA3 pyramidal cells and interneurons) as well as their afferent inputs unaffected, because these structures are generated before birth (Hicks and d'Amato, 1966; Bayer and Altman, 1975). Either repeated (fractionated) treatments with lower intensity irradiation or single high dose can produce massive reduction in the number of granule cells.

Bayer et al. (1973) used the fractionated method and described locomotor hyperactivity, reduced spontaneous alternation in a T maze and retarded acquisition of a passive avoidance task in rats with early radiation-induced hippocampal damage. Others reported on long bouts of spontaneous turning in a bowl apparatus (Mickley et al., 1989), enhanced acoustic startle responses (Mickley and Ferguson, 1989), impaired learning in the Morris water maze (Mickley et al., 1992) and showed that behavioral deficits caused by radiation-induced hypoplasia may progressively change during the maturation of the lesioned rats (Mickley et al., 1989).

To our knowledge no behavioral studies examined the effect of the single high dose of X-irradiation. The advantage of this method is that adequate timing of the treatment during the first 3 days of postnatal life

allows controlling the number of granule cells, and thus to determine the granule cell loss and the correlated behavioral deficit.

Other insults may also result in „selective" dentate gyrus lesions. Goldschmidt and Steward (1980) showed supersensitivity of hippocampal granule cells to toxic effects of the antimitotic alkaloid colchicine. Small, local injections of the appropriate concentration of colchicine into the dentate gyrus resulted in a dramatic loss of granule cells. It should be noted that colchicine-induced lesion always involves a severe destruction of the hilar region and the CA3 subregion of the Ammon's horn. Adrenalectomy is an alternative way of selective and noninvasive destruction of granule cells, because these cells apparently need adrenal hormone receptor stimulation to remain viable (Sloviter et al., 1989; 1993).

While colchicine and adrenalectomy in adult rats destroys already established structures, neonatal X-ray irradiation prevents formation of granule cells and related circuits. This substantial difference suggested the proposal that the neonatal lesion of the dentate gyrus of the rat can be a useful model to study pathological development of the related neural structures and the new findings may help understanding neurodevelopmental disorders.

The experimental work presented here is related to three fields:

a) **Anatomy:** investigation of the morphological consequences of the neonatal insult explored further details of the histology of the irradiated hippocampus (described in Chapter 2.).

b) **Electrophysiology:** reexamination of the kainic acid induced hyperexcitability of CA3 pyramidal cells in slices cut from irradiated hippocampus, revealed new quantitative relations between microelectrophysiology and anatomy of slice preparations. (described in Chapter 3.-4.).

c) **Behavior (spatial learning):** Tests on consequences of the neonatal insult in the Morris water maze of unilaterally and bilaterally irradiated rats (described in Chapter 5.-6.).

# Chapter 2.

# HISTOLOGICAL EVALUATION OF THE IRRADIATED RAT HIPPOCAMPUS

## INTRODUCTION

Previous detailed anatomical studies of the morphology of the neonatally irradiated hippocampus (e.g. Bayer and Altman, 1975; Dessi et al., 1991; Represa et al., 1991; Gaiarsa et al., 1992) described the effects upon the principal cells, without evaluation of the fate of interneurons. The traditional assumption on radiosensitivity of the multiplying cells (Altman et al. 1969) was supported by the demonstration that neonatal irradiation affect mainly the granule cell population (Bayer et al., 1973), while less obvious changes of other (e.g. pyramidal cells and interneurons) cell groups and afferent inputs were ignored since structures generated before birth (Hicks and d'Amato 1966, Bayer and Altman 1975) and were supposed to be X-ray resistant. However, Represa et al. (1991) reported a 60% reduction in the number of CA1 pyramidal cell population after neonatal irradiation.

Interneurons have crucial role of inhibition and regulate complex interactions among principal cells (e.g. Freund and Antal, 1988; Buzsaki, 1989; Freund et al., 1990; Miettinen et al., 1993). Immunhistology and NADPH-d histochemistry are well known methods for labeling and identifying various subpopulations of the GABAergic interneurons (see recent review by Freund and Buzsaki, 1996). As Kotti et al. (1997) pointed out, analysis of possible changes of interneurons is required together with determination of major principal cell losses.

The present study gives therefore a detailed anatomical description of the irradiated hippocampus, focusing especially on the interneurons. We applied the NADPH-d histochemistry and immunhistology using calretinin (CR), somatostatin (SOM) and parvalbumin (PV) antisera, combined with cell counting techniques to investigate the vulnerability of these specific classes of interneurons.

Although this short introduction contain points relevant in all subsequent chapters, it seems practical to avoid repetitions, and describe them only once.

# MATERIALS AND METHODS

For practical reasons, "Methods" sections of all subsequent chapters will contain only minimum information different from the generally applied techniques described here.

## Animals

Long-Evans hooded rats obtained from the Charles River Breeding Laboratories were used. The rats were kept under standard conditions with light cycle of 12 hour dark, 12 hour light and free access to lab chow and water. Pregnant females were isolated. Six to 12 h after birth, pups were taken for the X-ray irradiation and were returned immediately afterwards to their mothers. Loss of the hair on the head of the pups after the 10th postnatal day indicated the location and effectiveness of the irradiation. At least two irradiated rats together with two control littermates were used in each histological method.

## X-ray irradiation

Under light ether anesthesia pups were slipped into a lead-coated tube, which covered the whole body, with a circle of 5 mm in diameter over the middle of the cranium that corresponded the bilateral location of the dorsal hippocampi. X-rays (generated by a 60kV therapeutical equipment) were delivered dorso-ventrally. In most cases pups received a total dose of 6 Gy X-ray irradiation (1.2 Gy/min for 5 min). Differences will be indicated in the relevant chapters later. Single high dose was preferred instead of repeated irradiation over a period of several days with lower doses, because an early irradiation at 6 to 10 hours after birth destroyed all of the mitotic germinative cells and only 20 percent of granule cells remained. Therapeutical X-ray has low penetration rate in living tissue, therefore the ventral part was less affected than the dorsal hippocampus.

Please note, that throughout in this work the term "irradiated brain, hippocampus, slice, section, cells" will extensively be used to refer to tissue coming from irradiated rats, ignoring the fact that neonatal pups - and not tissue used from their brain several weeks later - were exposed to X-ray.

**Histological procedures**

Under deep ketamine anesthesia, animals were perfused transcardially first with 100 mM phosphate-buffer (PB) for 2 min and then with 500 ml of fixative containing 4% formaldehyde in PB (pH 7.4), for 30 min. The brains were removed from the skulls, postfixed for 1 h in fresh fixative solution and coronally sectioned on Vibratome at 50 μm, preserving the sequential order of the sections.

*NADPH diaphorase histochemistry.* After extensive washing, the free floating sections were incubated in a phosphate-buffered (100 mM PB) solution containing 0.1% NADPH, 0.02 % Nitroblue Tetrazolium and 0.3 % Triton X-100 (all reagents from Sigma) at 37 °C. The incubation were interrupted with several gentle shaking and the appropriate staining time was checked under light microscopy. The best results were obtained between 90-120 min of incubation. The slices were then washed in PB and mounted on a glass slide coated with gelatin. The sections were dehydrated in graded series of ethanol, cleared in xylene and covered with DePex.

*Immunocytochemistry.* After extensive washes sections were preincubated for 60 min at room temperature in blocking solution containing 10% normal goat serum, 0.5% Triton X-100 in PBS. Sections were then incubated for different antigens in rabbit anti-calretinin (1:2000), mouse anti-parvalbumin (1:2000), rabbit anti-somatostatin (1:1000) at 4 °C for two days. The second layer was goat anti-rabbit (1:200) or goat anti-mouse (1:200). Phosphate-buffered saline (100 mM PB, pH 7,4) containing 1% normal goat serum was used for washing. Sections were processed according to the ABC method using Vectastain Elite ABC Kit. After rinses in PB sections were incubated in a DAB kit (Vector / DAB, Peroxidase

Substrate Kit) at room temperature. The slices were then washed, mounted on a glass slide, dehydrated, cleared and covered.

*Cresyl Violet.* To determine total cell loss in the entire septo-temporal hippocampus, the brains were removed after perfusion, embedded in paraffin and serially sectioned at 10 μm thickness. The surface of the granule cell layer were measured in every fifth sections of the series. Cell density was calculated in 4 representative 10 μm thick Cresyl Violet stained sections (2 at the midseptal and 2 at the temporal level), in the granule cell layer of the dentate gyrus and in the pyramidal layer of the CA3/c area of each four rats. Then the averaged cell density (neurons / $\mu m^3$ x $10^6$ ) values were used to convert surface area data to estimation of total cell numbers.

*Timm's staining* (Timm, 1958) was used to show the mossy fibers in irradiated and control rats. Rats were perfused with buffered 1.2% sodium sulfide solution for 5 minutes, followed by 3% glutaraldehyde for 20 minutes. As a final step the animals were perfused again with sodium sulfide for 15 minutes. Removed brains were postfixed in 3% glutaraldehyde for 5 days, serially sectioned with the aid of a Vibratome at 50 μm and sections were mounted on gelatin-coated slides. On the following day sections were incubated in Timm's developer that contained gum arabic and silver nitrate according to the description by Danscher and Zimmer (1978). After 30 to 45 min of incubation at 37°C in dark, the reaction was stopped in 1% thiosulfate. Sections were counterstained with Cresyl Violet and covered by DePex.

*Intracellular labeling, tissue processing.* To mark functionally characterized cells for subsequent morphological investigation, micro-pipettes were filled with 2% biocytin (Sigma), dissolved in 1 M K- methyl sulphate, were used. After completing the physiological tests, 1.0 nA 400ms depolarizing pulses were passed every 600 ms for 5-15 min before the pipette was withdrawn from the cells. Slices were left in the recording chamber for an additional 15-30 min to allow for biocytin transport toward distal branches and were then sandwiched between layers of filter paper soaked in fixative in a phosphate-buffered solution (0.1 M PB, pH 7.4)

containing 4% paraformaldehyde (12 hr at 4 °C ). Slices were then cryoprotected in 10-20% sucrose in 0.1 M PB, flattened, frozen and sectioned on the freezing microtome at 60-80 μm. After several rinses in 100 mM PB, sections were processed with an ABC solution (1:25 Vectastain Elite / ABC Standard Kit) for 12-16 hr, washed in PB for 30 min, and incubated in DAB (Vector / DAB, Peroxidase Substrate Kit) for 15 min, washed in PB, and mounted on gelatin coated glass slides, dehydrated (in 50, 70, 80, 95, 100% ethanol), cleared in xylene and covered with DePex.

*Reconstruction of labeled neurons.* Camera lucida drawings were made from a few cells using an Olympus BX50WI microscope with a x40 dry or x100 oil immersion objectives. Axons were distinguished from dendrites by their smaller diameter, lack of spines, and continuity with the initial segment. Drawings were used for illustration purposes. For quantitative analysis a Nikon microscope with a x40 objective of and the Neurolucida software (see below) was used. The total dendritic length was traced and the number of branching points was determined. Although the dendritic arborizations of the best-stained cells are quite extensive, it must be noted that in 400 μm hippocampal slices processes were unavoidably cut. We calculated the number of thorny excrescences per section, and summed them to determine the total number of thorny excrescences per neuron.

*Cell counting and volumetry.* Quantitative analysis of the histological results was done with the help of the Neurolucida software (Neurolucida Version 2.0, Microbrightfield). Histochemically marked neurons, like NADPH-d positive cells were counted in every odd coronal sections of a serially cut hippocampus. The different subregions of the hippocampus were outlined and the NADPH-d containing cells were marked. The counted cells of the different subregions were then summed and multiplied by two to get the final number of NADPH-d positive cells.

Sections showing satisfactory immunochemical reactions were selected. A total of 20 sections from four different rats (five section per

animal) were used. Hippocampal and dentate gyrus CR, SOM, PV reactive neurons were counted at midseptotemporal level.

For volumetric analysis Cresyl Violet and Timm stained material were used. The area of the granule cell layer and mossy fiber bundle was measured in serial coronal sections covering the entire hippocampus. The computed areas of each outline were summed and the results from irradiated animals were compared to the mean values obtained from control non-irradiated littermate rats to reveal the magnitude of volumetric loss.

## RESULTS

Note, please, that main morphological findings discussed in subsequent chapters are described only once here.

Irradiated brains exhibited the following consistent histological changes: (1) marked loss of granule cells in dorsal and ventral hippocampus, with relative sparing of other classes of hippocampal neurons (see below); (2) slight or moderate decrease in size of hippocampal formation, with a related increase in size of the lateral ventricles; and (3) in the most severely irradiated animals, a shrinkage of the corpus callosum and the parietal cortex.

Reduction of the surface and total volume of granule cell layer and diminution of cell density in the dentate gyrus is shown in (Fig. 2.1.). More granule cells were eliminated in the septal half of hippocampus (about 70-80% loss), than in the temporal half (about 30-50% loss). Cell density of the granule cell layer was homogeneous along the septo-temporal axis in the control animals, but on the contrary, it was markedly reduced (by 45%) at the septal level of the irradiated hippocampus. Cell density was also smaller than control values in the temporal dentate gyrus of the irradiated hippocampus (by 30%). Further details on quantitative data is given in Chapter 4.

The thickness of CA3 pyramidal cell layer and the density of CA3 pyramidal cells in the irradiated hippocampus did not differ from the control, in contrast the CA1 region was clearly affected by the treatment and

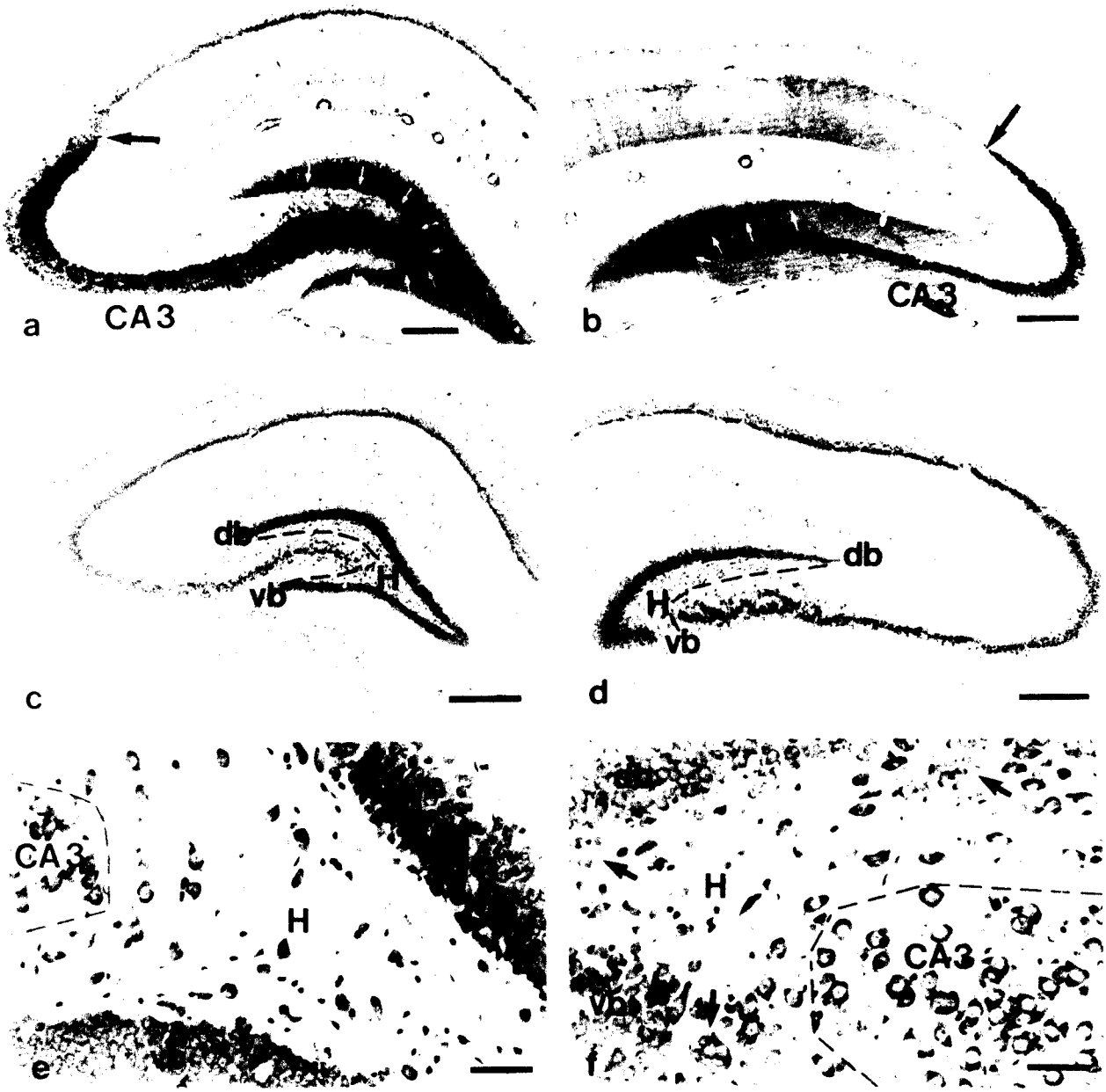


**FIGURE 2.1.** Photomicrographs of Timm (*a,b*) and Cresyl Violet (*c-f*) stained sections of the hippocampus in control (*a,c,e*) and X-ray irradiated (*b,d,f*) animals. *a,b*: Slight diminution of the mossy fiber bundle seen as a dark area outlining the hilus (white arrows) and the stratum lucidum of the CA3 subfield up to the border of CA2 area (large arrows). *c,d*: Both dorsal (db) and ventral blades (vb) of the dentate granule cell layer are shorter in the irradiated animal and the shape of hilus (H) has been changed. Bar = 400μm.

the pyramidal cell layer was wider in irradiated animals than in controls, but no systematic cell counts were done in the CA1 region.

**The number of hilar cells**

The hilus was smaller in irradiated animals (Fig. 2.1. *b* and *d*) than in controls and contained a number of non-aligned granule cells (Fig. 2.1. *f*). Although cell density appeared to be higher in the hilus of irradiated than that of the control animals (Fig. 2.1. *e* and *f*), systematic cell count of hilar neurons revealed a significant decrease after irradiation (Table 2.1.). The substantial reduction in the number of hilar neurons in the irradiated animals was disproportional (Table 2.1.) in respect of septo-temporal distribution. In the temporal hippocampus, 35% volume reduction of the granule cell layer was associated with a 20% decrease of the hilar cell population. However, in the septal hippocampus, where the volume of granule cell layer was reduced by 70%, the reduction of the number of hilar neurons was also larger (35%) than in the temporal half. The number of hilar cells in control animals given in Table 2.1. was similar to the number published before (35 000, Seress, 1988).

**Table 2.1**

Total number of hilar neurons in the control and X-ray irradiated rats*

| groups | animals | Septal hippocampus | Temporal hippocampus | Entire hippocampus |
|---|---|---|---|---|
| Control | No. 1. | 15.200 | 17.400 | 32.600 |
| | No. 2. | 15.600 | 17.800 | 33.400 |
| Irradiated | No. 1. | 9800 | 14.500 | 24.200 |
| | No. 2. | 9700 | 13.400 | 23.100 |

*Numbers are rounded to the hundreds. Cell counts were obtained from 2 control and 2 irradiated rats. Neurons were counted in each of the sections, applying the dissector method, where split cells at the upper surface of the sections were omitted.

**Parvalbumin immunoreactivity**

As previously reported (e.g. Kosaka et al., 1987), practically all cell bodies are located in strata pyramidale and oriens of the hippocampus and in

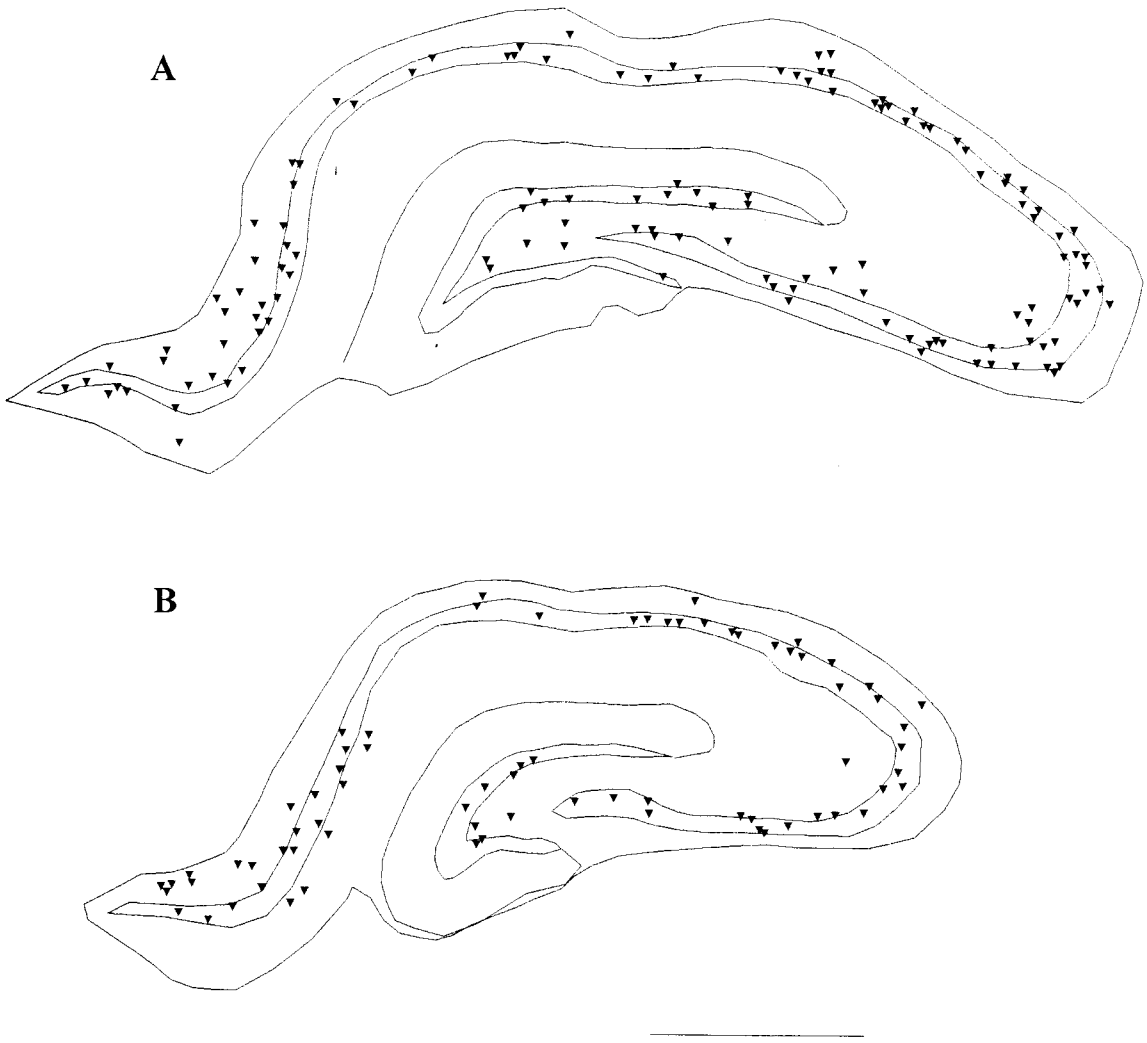


**FIGURE 2.2.** Neurolucida drawings illustrate the distribution of parvalbumin immunoreactive neurons in the control (A) and irradiated (B) hippocampi. Drawings represent single 50-μm-thick Vibratome sections, cut from approximately the same antero-posterior level of the hippocampus. Bar = 1200μm.

stratum granulosum and hilus of the dentate gyrus (Fig. 2.2.). In the dentate gyrus, more than 50% of the somata are in stratum granulosum, slightly less in the hilus, and only 2-3% in stratum moleculare. In the CA1 and CA3 subfields, the quantitative data are similar. More than 50% of the PV-immunoreactive cell bodies are in stratum pyramidale. 30-40% in stratum oriens, and only 3-6% in stratum radiatum.

There was a substantial reduction in the number of PV-immunoreactive neurons in the irradiated hippocampi (Table 2.2.). In the fascia dentata the cell number reduction was 20-30%, in the CA1 region cell number was decreased by 10-20%, whereas in the CA3 region there was no decrement (Fig. 2.2.).

**Table 2.2.**

The amount of cell loss among different type of interneuron subpopulations

| | Fascia Dentata | CA3 | CA1 |
|---|---|---|---|
| NADPH-d | 70-75% | 30-50% | 30-40% |
| PV | 20-30% | 0% | 10-20% |
| CR | 40-60% | 0% | 0% |
| SOM | 10-20% | 0% | 10-20% |

The irradiation induced cell loss in various subpopulations of GABAergic interneurons. The cell counting were obtained from 3-5 irradiated animals and the decrement is expressed relative (%) to the control ($n$ = 2 animals ) values.

**Calretinin immunoreactivity**

Immunostaining for CR reveals a large number of interneurons in all layers and subfields of the hippocampus and dentate gyrus (Jacobowitz and Winsky, 1991; Gulyás et al., 1992; Miettinen et al., 1992). In our samples we observed 40-60% decrease of CR labelelled neurons in the fascia dentata, whereas in the CA3 and CA1 region the number of CR immunoreactive neurons did not change (Fig. 2.3.).

**Somatostatin immunoreactivity**

The distribution and morphology of the somatostatin-containing neurons in the hippocampus followed the same pattern as previously described (e.g.

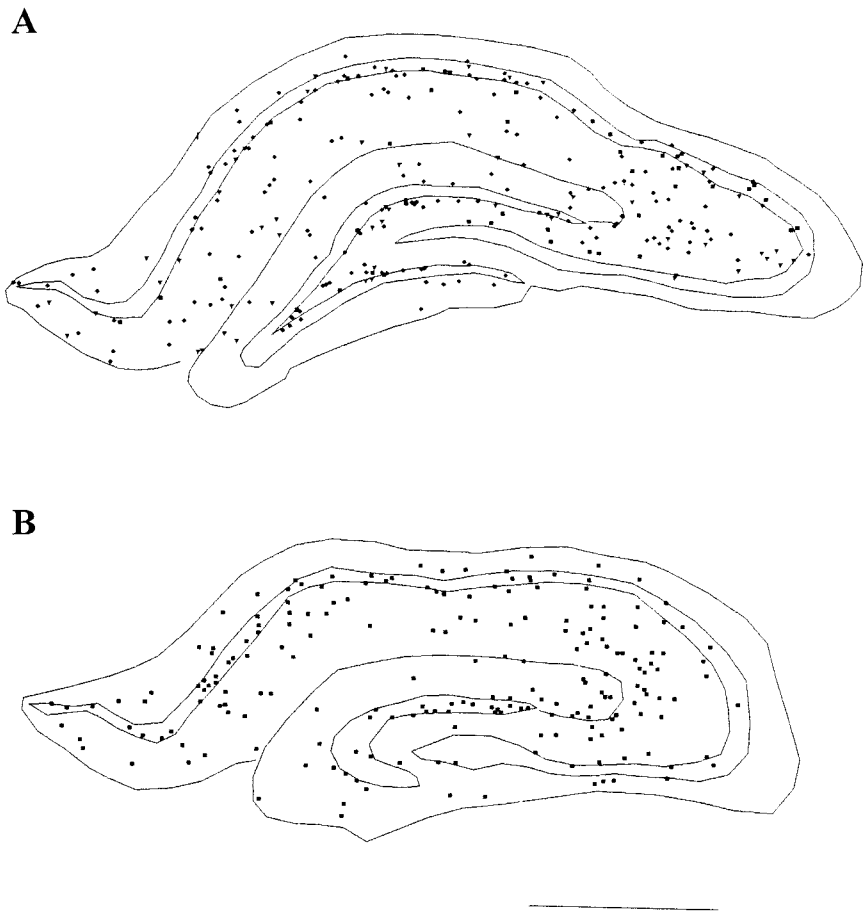


**FIGURE 2.3.** Neurolucida drawings illustrate the distribution of calretinin immunoreactive neurons in the control (A) and irradiated (B) hippocampi. Drawings represent single 50-μm-thick Vibratome sections, cut from approximately the same antero-posterior level of the hippocampus. Bar = 1000μm.

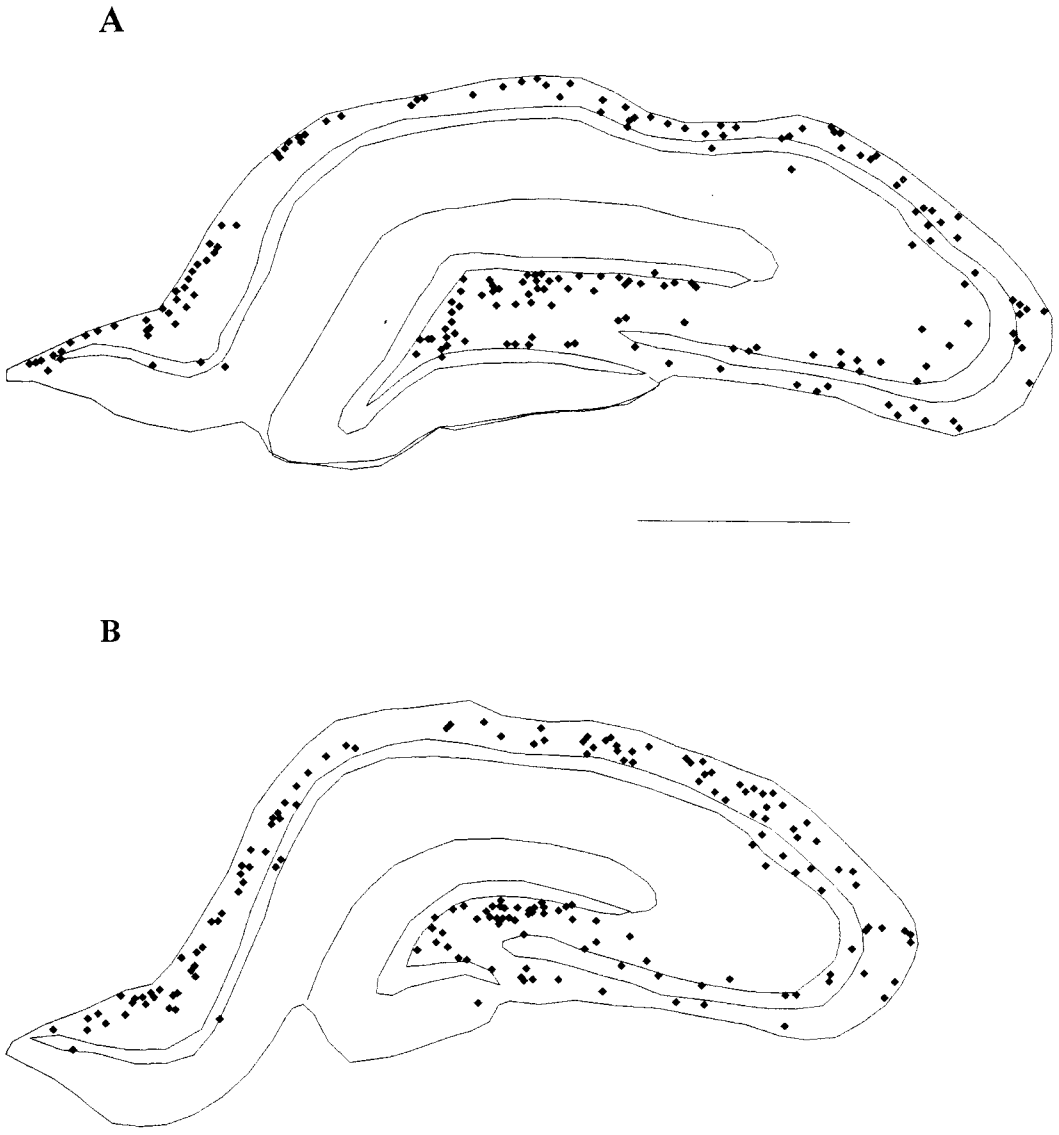


**FIGURE 2.4.** Neurolucida drawings illustrate the distribution of somatostatin immunoreactive neurons in the control (A) and irradiated (B) hippocampi. Drawings represent single 50-μm-thick Vibratome sections, cut from approximately the same antero-posterior level of the hippocampus. Bar = 1200μm.

Köhler and Chan-Palay, 1982; Johansson et al., 1984; Obata-Tsuto, 1987; Sloviter and Nilaver, 1987; Buckmaster et al., 1994). Briefly, immunstaining for SOM visualizes a large number of neurons in all subfields of the hippocampus, with characteristic laminar distribution. In the dentate gyrus, SOM-positive somata are restricted to the hilus, where they tend to accumulate in the subgranular polymorphic zone, but also numerous in the deep hilus and in areas bordering CA3c stratum radiatum. In the hippocampus, SOM-immunoreactive cell bodies are primarily confined to stratum oriens in the CA1 regions, with only a small number of cells in stratum pyramidale, and practically none in strata radiatum and lacunosum-moleculare. They are more widespread in the CA3 region and frequently occur in strata pyramidale, lucidum, and proximal radiatum.

Irradiation induced a substantial 20-30% loss of somatostatin-containing neurons in the hilus, and 10-20% decrease in the CA1 subfield (Table 2.2.), whereas somatostatin-containing neurons in the CA3 subfield were preserved (Fig. 2.4.).

**NADPH-diaphorase positive cells**

The distribution of NADPH diaphorase activity in the control hippocampus followed the same pattern as previously described (Vincent and Kimura, 1992; Valtschanoff et al. 1993). Briefly, the majority of the NADPH diaphorase-containing cells were located in the hilus of the dentate gyrus as well as in the stratum radiatum of the CA3 subfield. The other hippocampal areas had a moderate density of NADPH diaphorase cells, but they were rarely seen in the stratum lacunosum-moleculare of the CA1 area (Fig. 2.5.). Large amount of cell loss was observed among the NADPH diaphorase-containing cells. In the hilus the number of labelelled cells decreased by 70-75%, whereas 30-50% loss was observed in the CA3, and 30-40% in the CA1 region respectively (Table 2.2.).

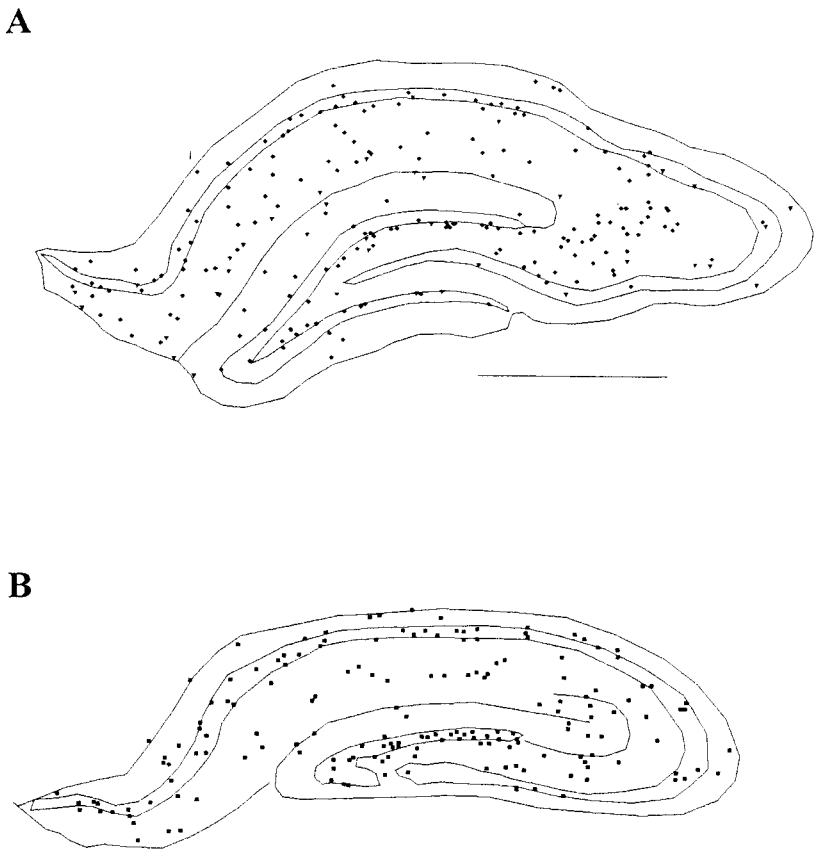


**FIGURE 2.5.** Neurolucida drawings illustrate the distribution of NADPH-d positive neurons in the control (A) and irradiated (B) hippocampi. Drawings represent single 50-μm-thick Vibratome sections, cut from approximately the same antero-posterior level of the hippocampus. Bar = 1000μm.

## DISCUSSION

The main finding of the present study is that the neonatal irradiation induced considerable amount of decrease among the various subpopulations of GABAergic interneurons in the hilus and in CA1 area, which accompanies previously reported histological damages.

Previous reports (Represa et al., 1991; Gaiarsa et al., 1992) did not describe significant loss of hilar neurons accompanying the granule cell loss. The changing shape of the dentate gyrus and an apparent increase in density of hilar neurons may give an impression that hilar cell number has not been changed. However systematic cell counts in Nissl stained material demonstrated a significant decrease in hilar cell number after irradiation. Additional immunostaining and NADPH-d histochemistry revealed that this reduction includes different neuronal cell types, including GABAergic and non-GABAergic cells.

This study investigated only a part of the various subpopulations of the hippocampal interneurons thus can not provide a precise estimation of the amount of total cell loss of interneurons. NADPH-diaphorase containing neurons represent about 30% of all GABAergic cells in the hippocampus (Czéh et al., 1997), whereas SOM-, and PV-positive cells account for 16%, and 20% respectively of all GAD-positive neurons in the in the dentate gyrus (Freund and Buzsaki, 1996). Thus the reduction of NADPH-d positive neurons to 30% in the hilus, accompanying with the 20-25% reduction of SOM-, and PV-positive cells altogether may represent a close estimate of 20-25% loss of all hilar GABAergic interneurons. Although Dun et al. (1994) and Nomura et al. (1997) reported substantial amount of co-localization among NOS and SOM neurons (also NOS and CR co-localization [Megias at al., 1997; Nomura et al., 1997]) , this estimation still might be correct considering the fact that the number of CR-positive neurons also reduced by 40-60%. Data about the proportion of GABAergic neurons that contain CR is not available (Freund and Buzsaki, 1996).

As expected the greatest amount of cell loss was detected in the hilar region, whereas except the NADPH-d positive neurons, no cell loss was

seen in the CA3 region. This data suggest, that the reduction of granule cells strongly affect the population of the hilar inhibitory cells, and it is likely that the reduction of interneurons is a consequence of the principal cell damage. This disruption of the anatomical integrity of the hilar region might substantially potentiate the damage on the function of the hippocampus, caused by the elimination of granule cells. Since hilar cells play a central role in the regulation of the input-output functions of the dentate gyrus (e.g. Amaral, 1978; Buzsáki et al., 1983) their loss might contribute to the behavioral deficits observed in the adult neonatally irradiated rats (see Chapter 5.-6.)

Interestingly the largest amount of cell reduction was observed among the NADPH-d positive neurons, as about 70% of these cells were lost in the hilus, and only this cell population decreased in the CA3 region, which suggest that this type of cell population is the most sensitive for this kind of lesion.

The mossy cells that form the other main subpopulation of the hilar region presumably were also decreased in their number, though these cells were not specifically identified .

The observed loss of interneurons of the CA1 area was unexpected, though Represa et al. (1991) reported that γ-ray irradiation reduces the number of pyramidal cells, and disturbs the developmental migration of surviving CA1 pyramidal cells. In contrast, in our preparations the CA1 region seemed to be only mildly affected by the treatment, but no systematic cell counts was performed. The detected interneuron loss argue that the anatomical integrity of the CA1 region was disrupted too.

Our results strongly suggests that irradiation affects not only the population of granule cells but also the interneurons, thus disrupting the anatomical integrity and presumably the function of the entire hippocampus, especially the closely related hilus. It is not yet clear whether the reduction of interneurons is a direct result of irradiation or a consequence of the principal cell damage.

Chapter 3.

# ELECTROPHYSIOLOGICAL CHARACTERISTICS AND MORPHOLOGICAL PROPERTIES OF DENTATE GRANULE- AND CA3 PYRAMIDAL CELLS IN SLICES CUT FROM NEONATALLY IRRADIATED RATS

## INTRODUCTION

Massive and permanent cellular loss induced at early postnatal life by irradiation may cause morphological changes in size, connectivity and organization of the remaining granule cells. Target cells may be expected to respond with morphological changes to substantial reduction of their mossy fiber (MF) input. Previous investigations (Represa et al., 1991; Gaiarsa et al., 1992) have indeed demonstrated modest shortening of the apical dendrites and slight morphological modification of the CA3 pyramidal cells, which were not affected directly by irradiation. In contrast, the morphology of surviving granule cells appears to be normal in Golgi preparations (Seress unpublished observation). In spite to the reduction of the target area (Chapter 2), the perforant path remains unimpaired with a large projection to similar location in the molecular layer of dentate gyrus (Seress and Freund, unpublished observation). It appears, therefore, that plastic changes in the hippocampus may occur in the input-output connectivity following removal of target cells before the establishment of synaptic connection. It remains possible however, that refined techniques can reveal less apparent changes both in the remaining granule cells and in their target neurons.

## MATERIALS AND METHODS

### Slice preparation

Under deep ketamine anesthesia, 3-6 weeks-old neonatally irradiated or control (non-irradiated) Long Evans rats of either sex, were perfused intracardially with 120 ml of ice-cold (1-4 °C ) oxygenated ACSF (artificial

cerebrospinal fluid) in which NaCl was replaced by 280 mM sucrose. The brains were quickly removed and immersed in the same solution. Coronal, 400 μm thick slices were cut using a Camden Vibroslice and the hippocampal formation was dissected out from the slice. Hippocampal slices were incubated first in the same solution allowed to warm up slowly, and after 30 min, they were transferred into pre-warmed (33-35 °C) ACSF containing (in mM): NaCl 124; KCl 3.5; $KH_2PO_4$ 1.25; $NaHCO_3$ 24; $CaCl_2$ 1.8; $MgSO_4$ 1.2 and were bubbled with a 95% $O_2$ and 5% $CO_2$ gas mixture to maintain pH 7.4, for further at least 1.5 hour of recovery. Slices were studied in a modified Haas type interface chamber, where they were perfused with ACSF (2 ml/min) and supplied with humidified carbogen at a temperature of 35 °C.

**Electrophysiology**

Electrodes for intracellular recordings were pulled by a horizontal puller (APP-1, Stoeltings) from borosilicate glass (resistance 120-150 MOhm) and were filled with 4 M K-acetate. Signals were amplified (Axoprobe) and fed into an IBM compatible microcomputer through an AD converter board (Digidata 1200) at a sampling frequency of 10 kHz for storage and later analysis. Stainless steel monopolar electrodes were placed in the inner blade of the dentate gyrus, or to the hilus - CA3 str. lucidum border where most of the MFs were thought to run. Constant current pulses of 0.1-0.2 ms 10-150 μA were delivered via an isolation unit (Grass, SIU-6) and repeated with less than 1 per 10 sec rate. All records shown in this paper are from the cell body layer of either the dentate gyrus or from the CA3*c* or *b* area.

Full details of intracellular labeling, tissue processing, and reconstruction of labeled neurons are given in Chapter 2.

# RESULTS

## Morphology of biocytin labeled cells in irradiated rats

Morphology of the granule and pyramidal cells visualized with biocytin labeling is similar in irradiated rats (Fig. 3.1.) to that found in normal rats (e.g. Lorente de No, 1934; Tamamaki et al. 1984; Fitch et al., 1989; Claiborne et al., 1990). Neither size and location of cell bodies, nor orientation and pattern of dendritic arborization were found to be changed qualitatively and quantitatively after irradiation. Initial part of axons of biocytin labeled cells can usually be seen, but our data on branching and projection of labeled axons are fragmentary.

In contrast, both the number and the complexity of the large spines (thorny excrescenses, TE) on the proximal dendrites of CA3 pyramidal cells are dramatically reduced after irradiation (1-6 TE/neuron in irradiated, whereas 20-30 TE/neuron in control hippocampi). This finding can be related to or a consequence of the reduction of the granule cell population in irradiated rats, because TEs are the only targets of the large mossy fiber terminals of the granule cell axons.

## Converging excitatory input to impaled cells

Variation of presynaptic stimulus intensity affects number of presynaptic fibers recruited from a pool which projects to the impaled cell from the vicinity of stimulating electrode. Fine gradation of size of EPSP in correlation with stepwise increase or decrease of stimulus strength reflects large number of converging afferents, each with relatively small individual postsynaptic effects resulting in what is called composite EPSP.

Amplitude of composite EPSPs fell in a range of 1-34 mV with a much narrow (4-9 ms) half-width in our sample of impaled cells. Small EPSP maximums indicated low threshold of postsynaptic discharges. A loose correlation was found between threshold of action potential and intensity of presynaptic stimulation. Cells with lower (range between -50 and -60 mV) membrane potential fired more easily to weak presynaptic volleys. Parameters of the stimulating current alone was not accepted to

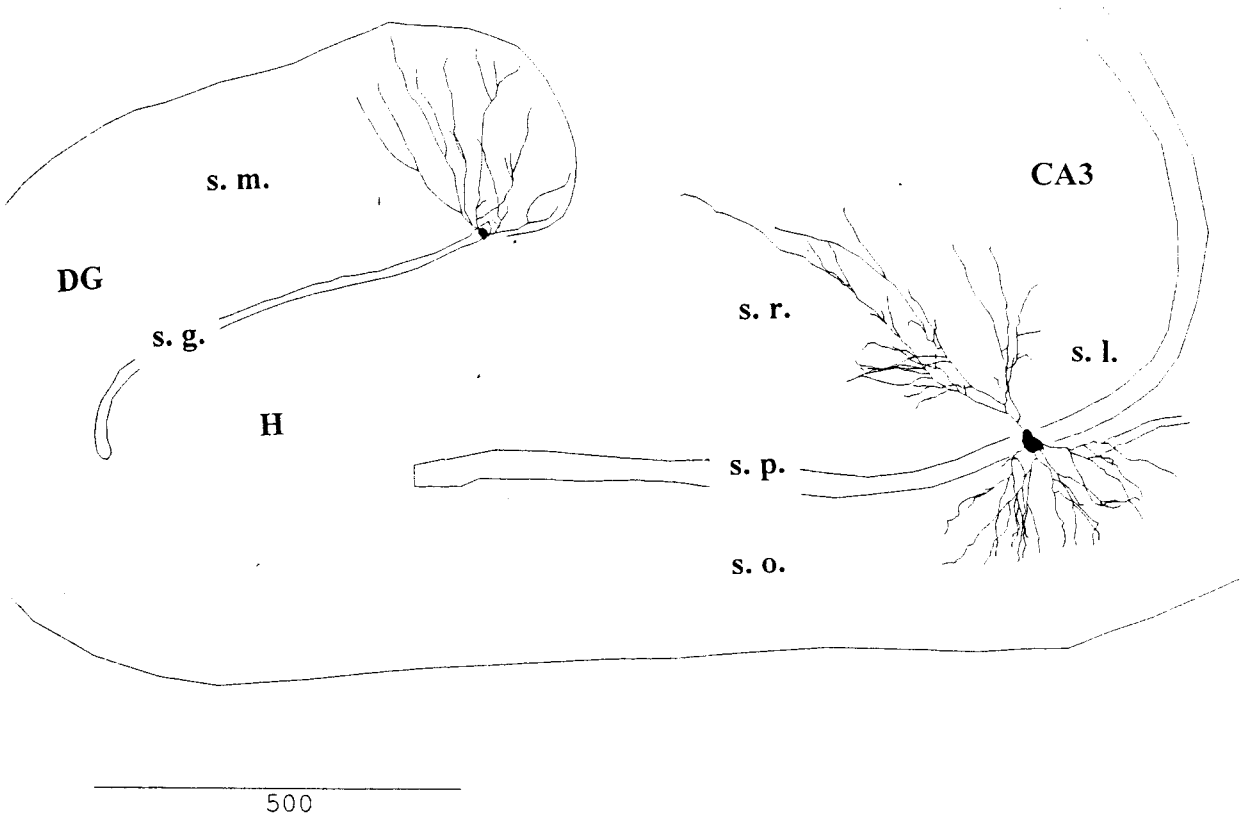


**FIGURE 3.1.** The dendritic arbors of a CA3 pyramidal and a granule cell filled with biocytin in a 400-μm slice in vitro from an irradiated, 6 weeks old rat, reconstructed from serial 80-μm sections. Scale bar = 500 μm.

judge the strength (efficacy) of presynaptic projection to any impaled cell. Across-cell and across-slice comparisons in data like firing threshold in term of stimulus intensity is obviously affected by factors like density of fibers at the site of stimulus, proportion of them projecting to the impaled cell and surviving the slice isolation techniques.

Two tests were used to estimate efficacy of excitatory inputs. Careful variation of stimulating current explored relative strength of stimulus intensity in correlation with evoked PSPs in the size range between barely detected and just sufficient to trigger an action potential. In the other test intracellular current injection was combined with variation of presynaptic stimulus intensity to examine how the evoked PSP was affected by the membrane potential of the postsynaptic cell.

The electrophysiological tests yielded ample evidence for the considerable convergence of a) both excitatory and inhibitory fibers, and b) both on dentate granule and CA3 pyramidal cells that were impaled. Representative illustration is shown in Fig. 3.2. from two pyramidal cells. The biggest subthreshold PSPs were about 10 times larger than the one to volleys just enough to induce some responses, or than the size of spontaneous EPSPs. Quite small differences were regularly seen between the peak amplitudes of individual EPSPs to moderate but slightly weaker or stronger volleys. Recordings like that are usually interpreted in terms of more or less presynaptic fibers recruited to the pool of stimulated ones on the assumption that more activated fibers would make the evoked EPSPs larger. The alternative explanation which considers variability of the amount of transmitter released from the same number of stimulated terminals, seems unlikely because small increase of stimulus intensity regularly makes the PSP larger. Amount of released transmitter in single terminals should not depend on stimulus intensity.

Similar gradation of the PSP in dentate granule cells was also observed. These granule cells had extensive but otherwise normal-looking dendritic arborization. Since irradiation does not destroy projective cells in the entorhinal cortex, the massive input arriving from the neocortex via the

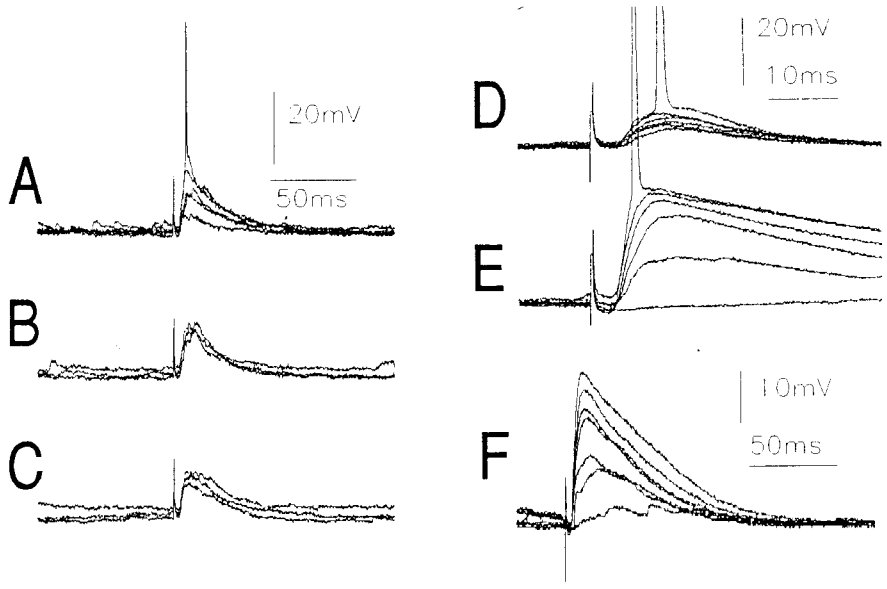


**FIGURE 3.2.** Graded composite EPSP responses to MF volleys evoked in irradiated CA3 pyramidal cells with various stimulus intensity. A-C: Spontaneous EPSP in this cell had similar size to the one evoked with the lowest intensity pulse in A. Note the small differences between sizes of EPSPs to moderate intensity volleys in B and C. D-F another cell. D: responses taken at -58 mV membrane potential (no current injection). E: responses to similar volleys at -75 mV membrane potential kept by current injection. The action potentials are clipped. F: Slower sweeps reveal time course of decay phase of postsynaptic potentials. Calibration in A refers also to B and C, while that in D refers also for E.

perforant path fibers must be processed by a substantially reduced granule cell population. However, in electrophysiological tests the input-output relationship of the perforant path-granule cell transmission appears to be similar in irradiated and in normal rats.

There was not even a single cell either in the dentate gyrus nor in the CA3 area which was unable to fire monosynaptic action potentials to a stimulation of the presynaptic fibers. This provides strong evidence for the considerable efficacy of presynaptic input in exciting the target cells. The approach in this study was not designed to detect small changes, if any, in the efficacy of synaptic transmission. The data firmly support two conclusions: 1) The large neocortical projection to a reduced number of granule cells in irradiated rats did not potentiate the relative strength of single or only a few fibers, because still a large number of presynaptic fibers had to be stimulated together to evoke postsynaptic discharges in granule cells. 2) The reduced MF projection toward CA3 cells remained sufficiently strong to induce postsynaptic discharges.

**Inhibitory components of the postsynaptic potentials**

Analysis of apparently simple composite EPSPs revealed masked IPSP components in many cells. This is a well-known property of CNS neurons. The term PSP was therefore preferred instead of the more specific EPSP and IPSP used only after exploration of the properties of the evoked responses. EPSPs were distinguished from IPSPs on the basis of reversal potential as shown in Fig. 3.3. Three practical guides were followed: initial (monosynaptic) EPSPs should reverse at around zero mV, a level of membrane potential never approached in our experiments, because depolarization induced repetitive firings. In depolarized cells AMPA-mediated EPSPs must be positive and usually smaller than those produced with the same presynaptic volley but recorded at higher (more negative) membrane potentials (e.g. Hestrin et al., 1990). Fast, presumably GABA-a receptor mediated IPSPs must show negative polarity at potential levels maintained sufficiently positive by current injection to induce regenerative

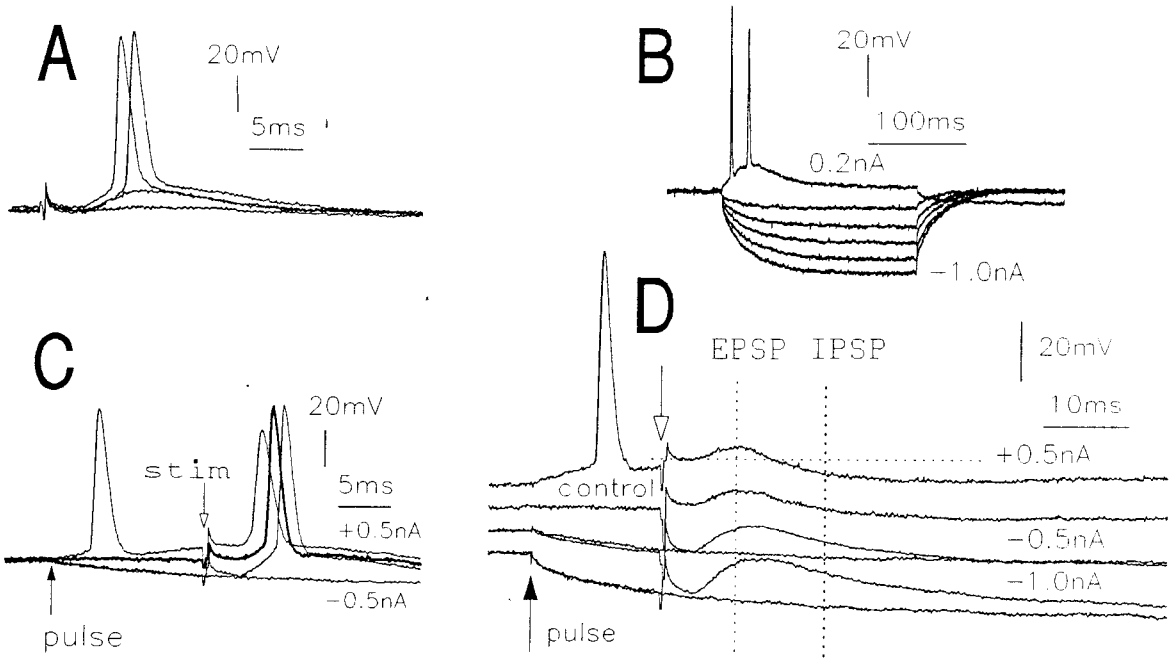


**FIGURE 3.3.** A: Four superimposed responses from a CA3 pyramidal cell evoked with 4 different presynaptic pulses in the range of 30 and 70 microA, 0.1 msec, to the hilus. B: Family of curves induced by intracellular current pulses varied in 0.2 nA steps between -1,0 nA and 0.2 nA. C: Initial portion of responses to similar intracellular current pulses combined with stimulation of the hilus with constant 70 microA intensity. In one of the four traces, depolarizing current was injected which itself induced an action potential, and reduced both the amplitude and the delay of the postsynaptic dicharge to the presynaptic volley. The second (thick) trace shows a control response, no current was injected. Hyperpolarization increased both the size and latency of postsynaptic discharge. D: Effects of current-induced shifts of membrane potential to the shape of PSP. The 6 responses are displaced to four levels for illustration purposes only.

firing of cells, since GABA-a mediated IPSPs should reverse at around -70 mV in ACSF used in our experiments (e.g. Mody et al., 1995). A second, much later and slower PSP component was also seen in many cells, which reversed at around 20-25 mV more negative membrane potential levels than early IPSPs. These late components were tentatively identified as GABA-b mediated IPSPs. Pharmacological tests with CNQX or bicuculline performed in some cells (not shown) supported fully the conclusions drawn from electrophysiological experiments.

Presumed IPSPs should inhibit excitations. Depolarizing current pulses was used to induce tonic firing of the impaled cells and the intensity of current was set to stabilize the rate of repetitive firing. Single presynaptic volleys sent toward the impaled cell were timed in a way that the presumed IPSP would occur during a period of current induced repetitive firing. Missing of action potentials were interpreted as evidence for the postsynaptic inhibition of the impaled cell (Fig. 3.4.).

Postsynaptic inhibition in the CA3 pyramidal cells requires activation of interneurons either in the hilus or in the CA3 subfield (Freund and Buzsaki, 1996). These presumed GABAergic cells are activated by the same MF bundle which excite the target pyramidal cells. Demonstration of IPSP component in pyramidal cells of irradiated rats provides therefore evidence for proper functioning of inhibitory circuits in spite of massive decrease and possible reorganization of projecting axons of granule cells.

**Biophysical properties of the cells in irradiated rats**

Time constant data, input output and I-V curves are available in the extensive literature of dentate granule and CA3 pyramidal cells studied in slices cut from normal rats (e.g. Scharfman, 1992). Quantitative details of the published measurements varied within ranges into which our data fit well. The ranges are rather wide and scatter of data may represent cells studied under slightly different conditions.

Resting membrane potentials were between -45 and -67 mV in the irradiated hippocampus. The input resistance measured at the end of the

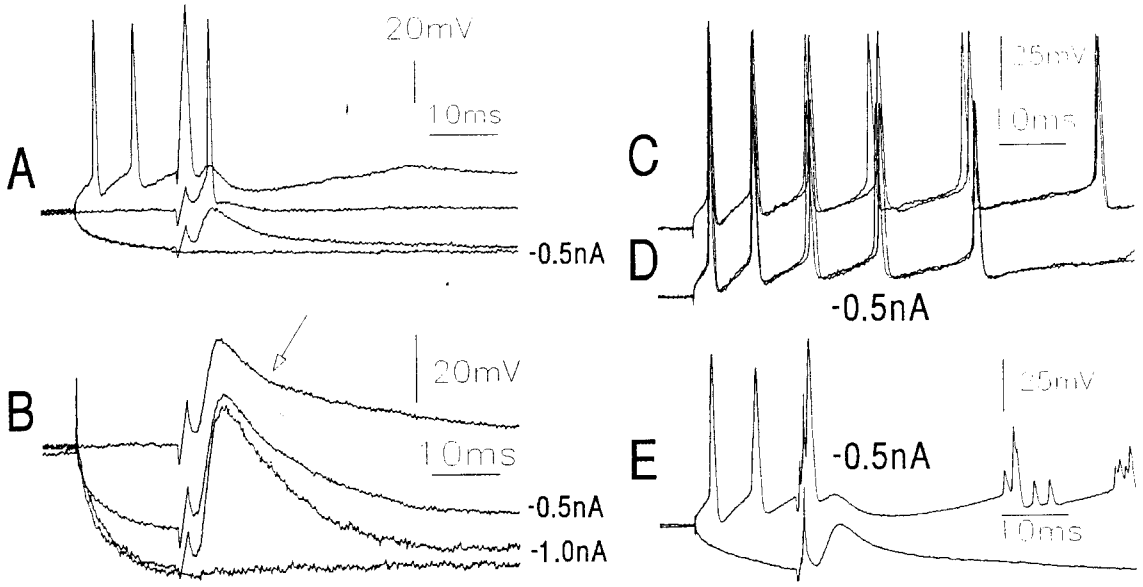


**FIGURE 3.4.** Evidence for IPSP-associated inhibition of firing in a dentate granule cell. All data from the same cell. A, top: response to a single molecular layer shock during a depolarizing (0.5nA) current pulse, which produces three action potentials and makes late component of PSP negative. Middle: control, response to the stimulus alone. Bottom two: current pulse with opposite polarity alone and together with the shock, now the late component of PSP is positive. B: PSP to reduced intensity stimulation. Arrow indicates presumed IPSP which is depolarizing at this membrane potential. Negative current pulses enlarge the PSP. C and D: several superimposed single sweeps show consistent rhythmic firing to 0.5 nA current pulses. E: Averages of 5 records. Upper trace a str. moleculare pulse evoked an EPSP-IPSP complex during the same current injections like in C and D. Note marked delay of the forth action potential. Bottom trace averaged responses to the opposite current and str.moleculare pulses.

voltage response to a 200 ms 0.5 nA hyperpolarizing current pulse delivered from the resting potential fell in the range of 20 to 75 MOhm. Time constant derived from responses to these pulses were 10-60 ms.

Size of action potential reached 94 mV, with a mean of monosynaptic action potentials to presynaptic volleys were 72 mV. Cells with less than 50 mV action potentials were rejected. Subthreshold volleys induced an EPSP-IPSP sequence. Representative measurements from 10 cells at near resting potential levels yielded 10-90 % EPSP rise time data of 3-5 ms, and half width data of 3-12 ms. All these properties were similar to those reported among others by Gaiarsa et al. (1994) and were therefore accepted as evidences for healthy conditions of the impaled cells.

## DISCUSSION

The main finding from the experiments presented in this chapter is that both orthodromic responsiveness, including contribution of GABAergic inhibition, and major biophysical parameters of the CA3 pyramidal cells and dentate granule cells remain quite similar in irradiated rats to those observed in control animals. Properties like action potential shape, duration, bursting, afterpotentials, as well as sensitivity of impaled cells and postsynaptic responses to current injections do not differ in cells impaled in irradiated from those found here or reported by others using non-irradiated animals. Morphological properties of the CA3 pyramidal and dentate granule cells are also similar to those seen in control animals, displaying similar dendritic length, spine morphology and spine density. These results suggest that afferent pathways to granule cells and pyramidal neurons do not show major rearrangement on the remaining target cells. This is valid in the connection between the granule cell - CA3 pyramidal cells, because after irradiation fewer thorny excrescences appear on the main apical dendrites of CA3 pyramidal cells. This suggests that remaining granule cells do not form additional thorny excrescences, although postsynaptic surface would be available. Possible changes like substantial increase of the strength of

synaptic transmission at individual contacts, which can compensate for the large reduction of the number of presynaptic cells, should not be excluded.

Efficacy or strength of synaptic transmission is an important parameter through which the nervous system can control information processing while anatomical organization of connectivity remains unaltered (e.g. Kuno, 1971; Redman, 1990; Bliss and Collingridge, 1993). At the level of cell-to-cell contact recent data (e.g. Gulyás et al., 1993; Halasy and Somogyi, 1993; Thomson et al., 1995; Cobb et al., 1997; Tóth et al., 1997; Acsády et al., 1998; Vida et al., 1998) provide evidence for considerable strength of transmission even at single boutons in the CNS. Note that the number of synaptic contacts between pairs of neurons studied simultaneously with intracellular recordings need subsequent morphological processing and involve labeling of both cells. Although projection of single cells may be strong enough to fire postsynaptic cells like for example in the climbing fiber - Purkinje cell contacts in the cerebellum, the majority of CNS neurons require considerable but unknown number of converging excitatory terminals to be activated near simultaneously to reach firing threshold.

Composite EPSP data shown here provide a strong evidence for convergence itself but demonstration of fine gradation suggests that slight difference in stimulus intensity affects size of postsynaptic response. Variation of stimulus intensity likely adjusts the number of stimulated presynaptic fibers, but not the probability of transmitter release at individual active sites.

As it is known the exclusive target of MF terminals on CA3 pyramidal cells are the giant spines also known as TE. Since the number of TE is considerably decreased after elimination of a large portion of MF fibers, one expects a decrease of probability of getting monosynaptic discharges of CA3 pyramidal cells by MF volleys. It was not the case, however, thus we conclude that the MF-CA3 transmission remains at least as efficient in irradiated than in normal MF-CA3 pyramidal contacts. At present we can not correlate the data from irradiated cells to the results of

quantal analysis performed in hippocampal cells (e.g. Jonas et al., 1993, Chicurel and Harris, 1992, Stricker et al., 1996, Schiller et al. 1998).

The limited biophysical data available from the labeled cells in our sample are not sufficient to judge possible changes in properties like electrotonic length of the dendrites, which can affect efficacy of synaptic transmission.

Postsynaptic inhibition demonstrated in granule cells of irradiated rats was evaluated as evidence for survival of postsynaptic inhibitory circuits projecting to the dentate gyrus. Inhibitory circuits projecting to either the CA3 or the dentate area remain efficient in irradiated animals in spite of the considerable decrease of the number of hilar cells (Chapter 2), suggesting that the relatively small decrease in the number of PV positive basket cells does not alter significantly the perisomatic inhibition. Our tests are not detailed enough to demonstrate a possible change in the dendritic inhibition due to the large loss of NADPH-d positive cells.

# Chapter 4.

# RESIDUAL GRANULE CELLS CAN MAINTAIN SUSCEPTIBILITY OF CA3 PYRAMIDAL CELLS TO KAINATE-INDUCED EPILEPTIFORM DISCHARGES

## INTRODUCTION

Kainic acid (KA), a toxic compound activates two pharmacologically defined types of ionotropic glutamate receptors. Kainate receptors, encoded by GluR5-7 and KA1-2 functional glutamate receptor subunits are more sensitive to KA than AMPA receptors assembled from GluR1-4 subunits. Density of kainate receptors is high in mossy fiber (MF) synapses, which are assumed to contribute mostly to the effects of KA applications. KA induces spontaneous recurrent paroxysmal activity (SRPA) and causes selective death in the hippocampus (Tauck and Nadler, 1985; Okazaki et al., 1988; Okazaki and Nadler, 1988; Nicoll et al., 1990; Sloviter, 1992). Mossy cells, CA3 pyramidal cells, calretinin- or somatostatin positive hilar neurons are especially vulnerable to acute excitotoxic conditions (Freund and Buzsaki, 1996). Excitotoxin sensitive cells receive heavy MF innervation from the dentate granule cells which themselves are resistant to KA toxicity. Mechanisms of SRPA induction and delayed excitotoxic destruction of hippocampal cells are not clear. A critical amount of MF innervation is needed to generate SRPA and toxic reactions for adult CA3 pyramidal cells, because such neurons in young rats are apparently resistant to KA-induced cell death (Wolf and Keilhoff, 1984; Sperber et al., 1991; Ribak and Navetta, 1994). Small amounts of applied KA fail to cause neuronal cell death but have been shown to induce convulsions both in vivo and in hippocampal slice preparations (Nadler et al., 1978; Westbrook and Lothman, 1983; Fisher and Alger, 1984; Ben-Ari, 1985; Benedikz et al., 1993). Ben-Ari and Gho (1988) have described details of the action of brief KA applications on CA3 area. Intracellular recordings reveal spontaneous as well as evoked bursts of several action potentials riding on a large slow depolarizing wave. The bursts have been attributed to facilitation of

excitatory and depression of inhibitory components of polysynaptic networks. Higher doses of KA depress the excitatory synaptic potentials and discharges.

Gaiarsa et al. (1994) have reported that KA fails to induce epileptiform discharges in the CA3 subfield in slices cut from neonatally irradiated rats. KA injected into the hippocampus or lateral ventricles of neonatally irradiated rats do not initiate degeneration of CA3 pyramidal cells (Gaiarsa et al., 1994). These findings support earlier reports on reduced probability of CA3 cell bursting in rats with surgical MF lesion (Okazaki et al., 1988). However, recent results in our laboratory suggest that KA remains toxic in adult animals in which approximately 80% of the granule cells are destroyed by neonatal irradiation, or even in animals where the MF bundle has completely been eliminated by colchicine injection two weeks before the KA treatment of irradiated rats (Horváth et al., 1995). The present study reports on KA induced epileptiform discharges recorded in many CA3 pyramidal cells in slice preparations from neonatally X-ray irradiated animals and suggest a quantitative relationship between the amount of remaining granule cells and the KA induced burst discharges.

## MATERIALS AND METHODS

### Slices

Methods of slice preparation were described in Chapter 3. After the electrophysiological recordings the effect of irradiation was verified applying the Cresyl Violet staining. At the end of the experiments, the slices were sandwiched between layers of filter paper soaked in fixative (0.1 M PB with 4% paraformaldehyde, pH 7.4) for a few minutes, than kept in fixative overnight. Since only one side of the hemisected brains were used to cut slices, the other half was also fixed and processed later. The fixed tissue of the slices used for electrophysiology and the opposite halves of the brain were embedded into paraffin and sectioned with sliding microtome. Every 10 μm thick section cut from the fixed slice, and every sixth serial section cut from the other hemisphere was mounted and stained with Cresyl Violet.

Calculation of the number of granule cells from density and area measurements for the entire septo-temporal length of the hippocampus in perfused brains (see Chapter 2.) provided sufficient background to judge effects of irradiation in coronal section samples taken from slices used for electrophysiology, or in some cases from the sections of the contralateral hemisphere. Estimation of irradiation induced cell loss from surface and cell density data was felt reliable even if tissue preservation in physiologically tested slices was weaker than that of the perfused animals. Surface area data were obtained from slices accepted for physiological analysis and from many sections of the contralateral hippocampi of irradiated rats. The granule cell layer was always preserved well enough for measuring its total surface.

**Electrophysiology**

Evoked field potentials were recorded with glass micropipettes filled with 150 mM NaCl (resistance 3-5 MOhm) in reference to a silver - silver chloride bath ground. Recording pipettes were positioned into the cell body layer of the CA3 region between the hilus and the fimbria. Sampling and MF stimulation was described in Chapter 3. The stimulus intensity was set to evoke a near maximal population spike amplitude. Population spike responses suggested that the tissue was able to generate waveforms sufficiently large to be detected when exposed to KA without electrical stimulation. This was important to know to avoid false negative conclusions concerning the effect of KA on SRPA. Periods of KA application was continuously recorded with the Axotape software (Axon Instruments Inc.) while the evoked responses were tested with 0.2 Hz rate and recorded in pClamp suite. Intracellular recording was described in Chapter 3.

Kainic acid (Sigma) was dissolved fresh in ACSF (300-500 nM/l) and applied to the bath using a three-way tap system. Slices were exposed to the drug for 5-6 minutes only. SRPA was seen during the first half of that period, and washing with control ACSF started when the depression of the evoked responses become obvious.

### Histological procedures

were described in Chapter 2.

## RESULTS

### Histology of the irradiated hippocampus

The detailed descriptions in Chapter 2 are completed here with data on volumetric analysis of the normal and irradiated hippocampus.

X-ray irradiation reduced the surface and total volume of granule cell layer (Figs. 2.1., 4.1.). However, the loss of granule cells calculated from the area measurements shown in Fig. 4.1. was greater in the septal half of hippocampus, than in the temporal half. The surface area occupied by the MF bundle was also reduced by irradiation both in the hilus and in the stratum lucidum of CA3 area (Fig. 2.1. *a* and *b*). The thickness of CA3 pyramidal cell layer and the density of CA3 pyramidal cells in the irradiated hippocampus did not differ from the control data (Fig. 2.1. *c* and *d*).

In the Timm stained material the mean area of granule cell layer in the septal hippocampus cut from the midseptal level (Fig. 4.1. A and B) was 0.290 ± 0.031 in control and 0.103 ± 0.023 in irradiated hippocampi (mean value in $mm^2$ ± S.D./section) corresponding to around 45% loss. Numbers obtained from the temporal part of the hippocampus were different: the mean area was 0.724 ± 0.087 in control and 0.584 ± 0.096 in irradiated hippocampi, reflecting only about 25% loss (Fig. 4.1. C and D). Cell density in paraffin embedded, Cresyl Violet stained sections was homogeneous along the septo-temporal axis in the control animals (1721 ± 84 neurons / $\mu m^3$ x $10^6$). On the contrary, cell density of the granule cell layer at the septal level of the irradiated hippocampus was markedly reduced (945 ± 105 neurons / $\mu m^3$ x $10^6$). Cell density was also smaller than control values in the temporal dentate gyrus of the irradiated hippocampus (1231 ± 124 neurons / $\mu m^3$ x $10^6$). As a consequence, reduction of areas indicated an even larger decrease in the number of granule cells of the irradiated rats. Either calculation revealed substantial difference between losses in the temporal and in the septal parts of the hippocampus.

The mean volume of granule cell layer in Timm stained controls ($n$ = 4) was 1.86 ± 0.01 $mm^3$ ± S.D. and that in irradiated rats ($n$ = 4) was 0.77 ± 0.22 $mm^3$ ± S.D. which indicated 60% reduction. The volumetric data measured in Cresyl Violet stained sections were numerically different because shrinkage is much larger in paraffin embedded brains than in those cut by Vibratome without embedding. Density and volume data together indicated a decrease of the total number of granule cells considered proportional with the decrease of the total volume. The estimated granule cell number for control obtained indirectly was close to the direct count published before (650 000, Seress 1988).

Smaller loss of surface area of Timm-stained MF bundles was observed in X-ray irradiated hippocampi than expected from the reduction of granule cells (Fig. 4.1.). While the surface of dentate granular layer in the septal half of the dorsal hippocampus was decreased to 30-40 percent, the surface of MF bundle was reduced to only 60% in the same region. The mean area of MF bundle in the septal hippocampus was 0.388 ± 0.032 in control and 0.220 ± 0.043 in irradiated hippocampi (mean value in $mm^2$ ± S.D./section). In the temporal half of the hippocampus the reduction was smaller because the surface area of MF bundle showed only 15% reduction (mean area was 0.495 ± 0.073 in control and 0.421 ± 0.123 in irradiated hippocampi).

**FIGURE 4.1.**
Surface area of granule cell layer and MF terminal zone as determined in Neurolucida from Timm stained coronal sections. The hippocampus was divided to septal (A) and temporal (C) halves at the Bregma -5.3 mm antero-posterior level according to Paxinos and Watson (1982). Neurolucida drawings (A to D) illustrate the different amount of reduction of granule cell layer (filled black area) and MF bundle (filled gray area) in the septo-temporal axis in control and X-ray irradiated animals. Drawings represent Timm stained coronal section at midseptal level of the hippocampus from control (A) and X-ray irradiated rat (B). Similar drawings at about 2.5 mm more caudal level from control (C) and irradiated (D) rats demonstrate that the area of residual granule cell layer were much larger in the temporal than in the septal level of the hippocampus of the irradiated rats. E: The sum of residual granule cell layer area computed from four individual irradiated rats (each animal is represented separately by a bar) is expressed relative to the mean control value (100%) obtained from intact rats ($n$ = 4). F: The residual MF bundle of the irradiated rats represented like the granule cell layer on E.

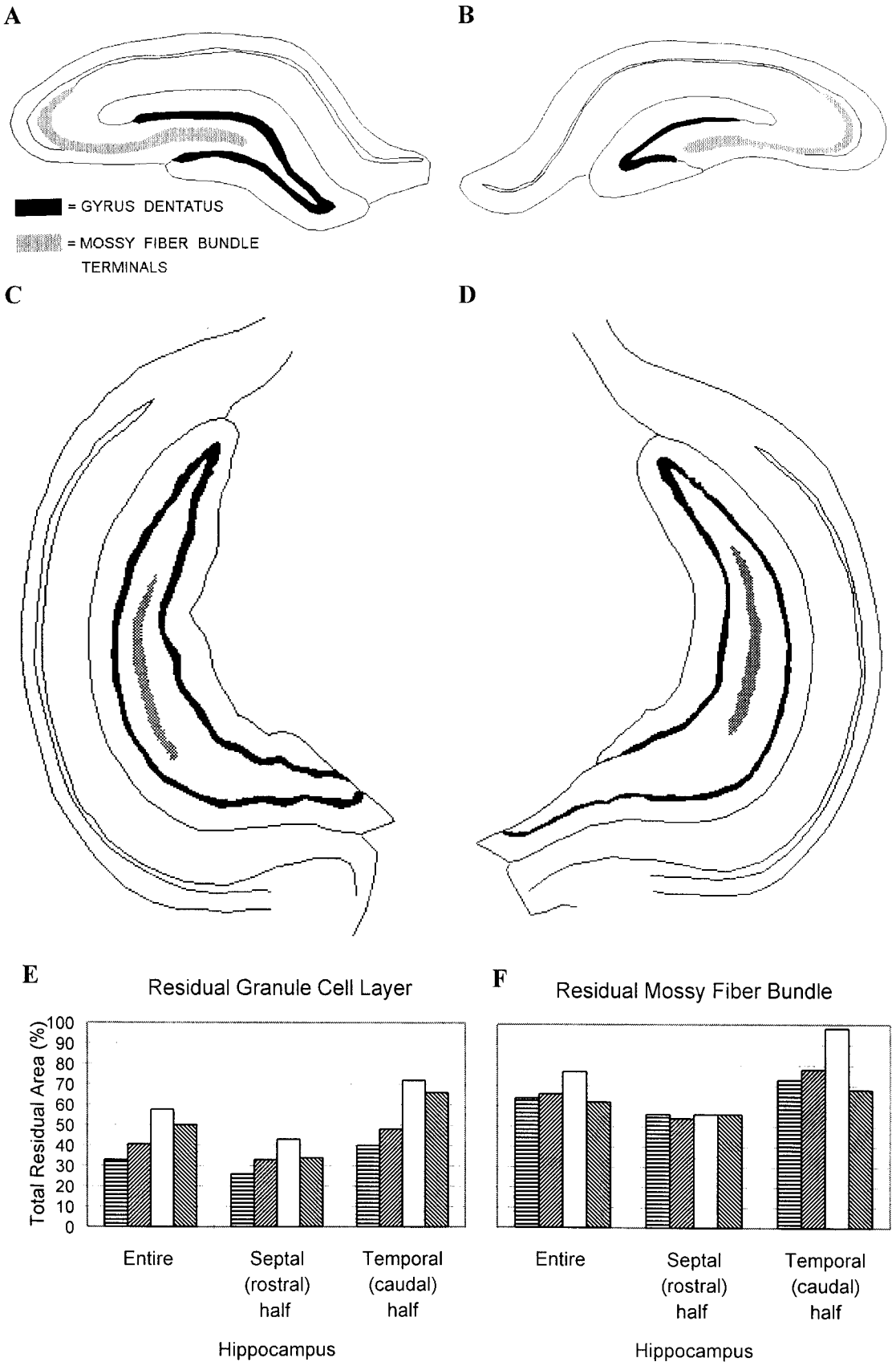
A
B
= GYRUS DENTATUS
= MOSSY FIBER BUNDLE TERMINALS
C
D
E
Residual Granule Cell Layer
Total Residual Area (%)
100
90
80
70
60
50
40
30
20
10
0
Entire
Septal (rostral) half
Temporal (caudal) half
Hippocampus
F
Residual Mossy Fiber Bundle
Entire
Septal (rostral) half
Temporal (caudal) half
Hippocampus

**FIGURE 4.1.**

**Extracellular recordings**

In 27 experiments, 22 slices from 8 normal rats and 46 slices from 19 irradiated rats were studied with electrophysiological techniques. Extracellular recording techniques were employed to analyze how irradiation and KA exposure affected the field potentials. Since consequences of bath application of KA were adequately described (e.g. Fisher and Alger, 1984; Ben-Ari and Gho, 1988) and our observations did not warrant revision of that knowledge, the data below served two purposes. First, to assess physiological condition of slices by electrical stimulation of the MF bundle. The 46 slices from irradiated rats were included because they all responded to MF volley with waveforms like the one shown in Fig. 4.2. and generated field potentials of at least 0.5 mV amplitude. Many of the slices rejected on the basis of poor responsiveness come from brains sorted among those in which more than 60% of the granule cell loss was verified histologically. The second purpose was to demonstrate that populations, not only a few CA3 pyramidal cells selected for intracellular recordings, could be activated by KA application to the bath in irradiated rats.

The amplitude of MF induced field potentials in the cell body layer of CA3 area of irradiated slices often remained below 1 mV (peak to peak) in the slices cut from the septal half hippocampus as compared with 2-4 mV observed in control slices. Since responses evoked in other areas (e.g. the CA1 pyramidal cell layer) were much larger and similar to those observed in non-irradiated preparations, small size of CA3 evoked potentials in slices from irradiated rats were attributed to loss of granule cells and the MF bundle, instead of poor health of the tissue. Since the stimulating electrode was in the hilus, in the vicinity to the residual granule cells, and the recording pipette in the CA3c area, a major portion of the evoked postsynaptic response could likely be generated by MF activation. No effort was made to separate presynaptic fiber volleys from antidromic activation of pyramidal cells via recurrent axon collaterals, or to identify excitatory CA3-CA3 interactions. These important issues could be ignored because our main concern was KA-induced activity which unlikely contained either

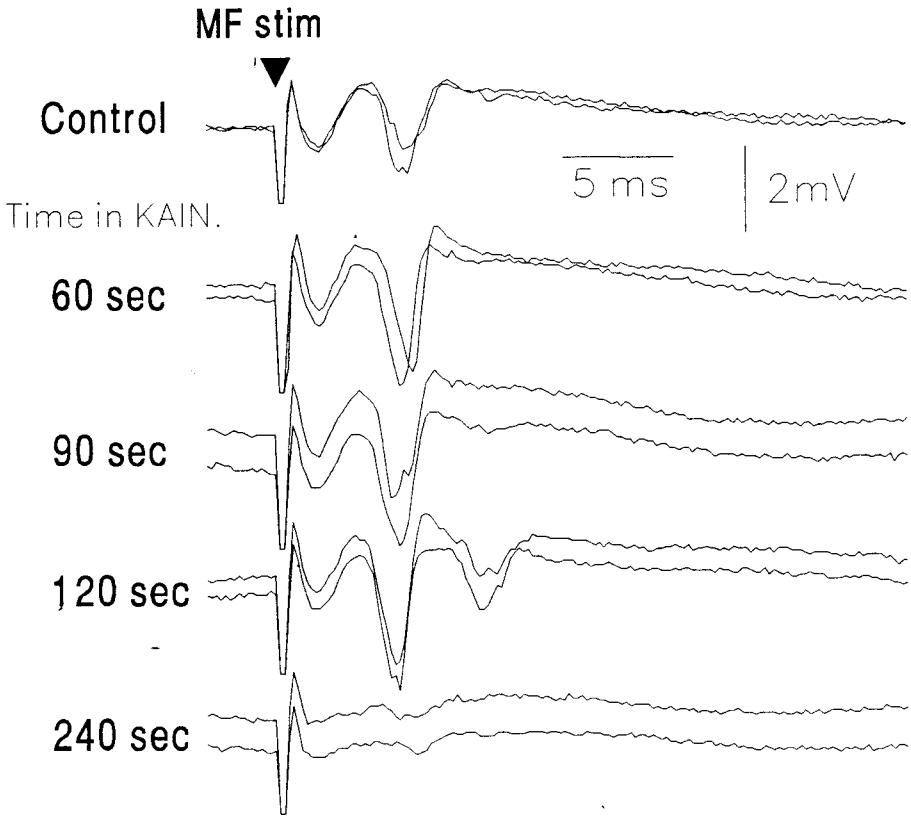


**FIGURE 4.2.** Changes of postsynaptic responses with KA application. Averaged (means of 4 sweeps each, two means superimposed in each rows) field potentials taken in the cell body layer of the CA3c area. Slice from the temporal half of the hippocampus of an irradiated rat. The MF bundle was stimulated with constant (100 μA) intensity. Calibration as indicated for all sweeps, negativity downward like in all figures of the present chapter.

antidromic or presynaptic volley components. Population postsynaptic potential (PSP) appeared as a positive wave from which a sharp negative spike with about 4-5 ms latency indicated that many postsynaptic cells were excited by and some pyramidal cells discharged to MF volleys.

Both in control and in irradiated slices KA first facilitated and subsequently depressed the evoked postsynaptic field potential responses. During 3-5 min KA exposure depression could be almost complete (Fig. 4.2.) but reversible in 20-30 min (not shown). Both the PSP and population-spike components were affected. Often a second or a third population spike followed the enlarged initial one during the facilitatory period. Periods of facilitation and occurrence of SRPA overlapped, but details of this time relationship were not examined. No difference appeared between irradiated and control slices in respect of these aspects of KA-induced changes.

Under the effect of KA, SRPA was seen for minutes in normal slices before depression become dominant. Approximate frequency of SRPA was 1-0.1 Hz (Fig. 4.3. A,B) in normal rats with electrophysiological properties similar to those published by others (e.g. Fisher and Alger, 1984). Bursts of population spikes in the CA3 area also occurred in some (6 studied only with extracellular recordings, and 12 others from which intracellular data were collected) irradiated slices, especially in those cut from the temporal half of the hippocampus (Fig. 4.3. C-F). Details of waveforms varied among normal and irradiated slices, but the prolonged (20-50 ms) slow positive waves in the cell body layer and the 5-8 negative population spikes emerging from them allowed identification of SRPA. Like in the case of evoked potentials, amplitude of both the slow wave and the population spike components of SRPA was smaller in irradiated than in normal slices. Frequency of SRPA tended to be lower in irradiated than in normal slices which hampered detection of them. For example data like 3-5 small SRPAs during a 2-3 min period might indicate that irradiation was effective in eliminating SRPA but also raised the possibility that a bit higher concentration of KA could produce more SRPA in that particular slice.

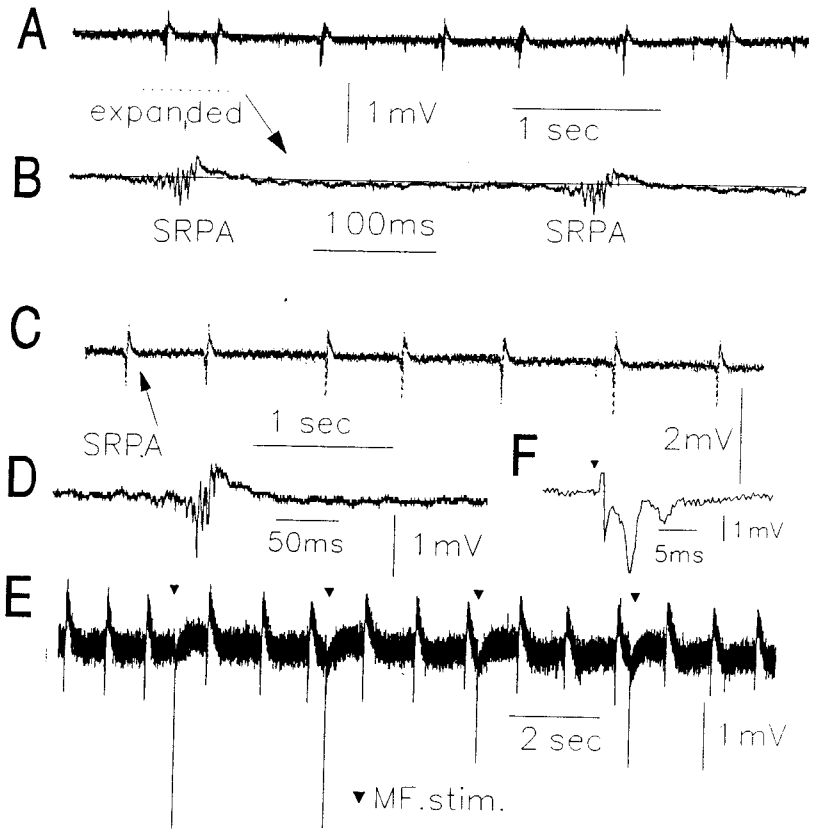


**FIGURE 4.3.** KA induced SRPA in the pyramidal layer of temporal CA3 area. Samples from periods with highest rate of SRPA taken from tape-recorded (sampling rate 5 KHz) episodes. Expanded sweeps show details of waveforms. A, B: Data from a normal rat in the third minute of KA (300 nM in the bath) application. The 1 mV bar applies for both sweeps. C,D: Similar data from an irradiated slice with 500 nM KA in the bath. E, F: MF-stimulus (triangles) evoked responses and 300 nM KA-induced SRPA in a slice from another irradiated rat. Neither slice showed spontaneous activity before KA application. The sample evoked response in F is about twice as big as the ones taken before KA application (not shown).

There were slices cut from irradiated rats in which KA failed to induce SRPA but provoked another form of spontaneous activity. Namely in 14 slices many small population spikes occurred more or less periodically, in other cases almost regularly, for 1-3 minutes in the presence of KA, and disappeared together with the depression of evoked responses. Similar activity was rarely observed in normal slices treated with KA. Finally there were slices in which KA quickly depressed all the evoked responses and spontaneous activity was neither expected nor found in them. Efforts to obtain more convincing data on SRPA in irradiated slices with slightly higher concentration of KA might cause the adverse effect in promoting faster depression of all activity.

Thus although irradiation decreased the likelihood of getting SRPA, clear examples of KA-induced SRPA in irradiated slices should be considered as underestimation of the effect of KA in promoting burst-firing in CA3 pyramidal cells, because poorly synchronized discharges of only a few cells would unlikely generate SRPA waves in extracellular recordings. Besides low frequency of SRPA combined with depression also induced by KA exposure made interpretation of data difficult.

**Intracellular recordings**

Cells impaled in the CA3 cell body layer were identified as pyramidal cells because they fired bursts to depolarizing current pulses and responded with monosynaptic discharges to MF volleys. Although these criteria alone are insufficient to exclude all types of interneurons (Freund and Buzsáki, 1996), it seems quite unlikely that all our cells with fairly similar electrophysiological properties were interneurons instead of pyramidal cells. In addition, several cells were labeled by biocytin and identified as pyramidal cells with strict morphological criteria (Chapter 3.).

Presumed pyramidal cells ($n$ = 55) impaled in slices cut 4 weeks after neonatal irradiation usually fired single action potential to MF volleys of suprathreshold intensity. Weaker volleys induced PSP waves considered as a mixture of an initial EPSP followed by either a depolarizing or a

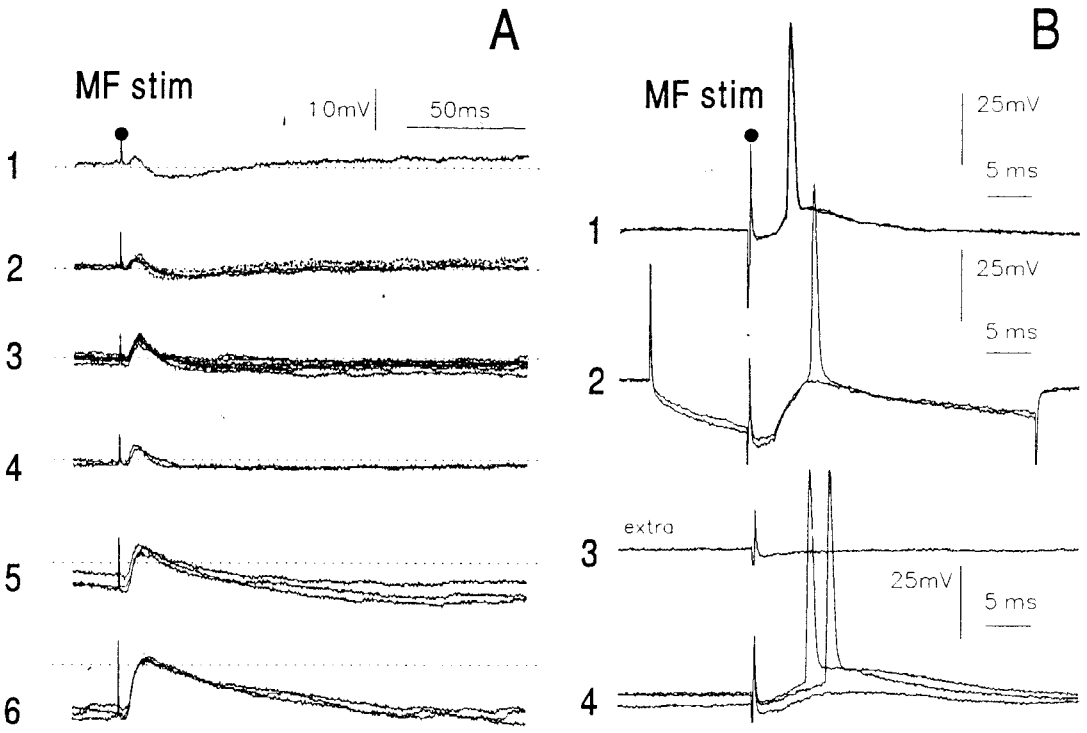


**FIGURE 4.4.** Changes of MF evoked responses in CA3 pyramidal cells at different membrane potentials set by current injection. Slice from an irradiated rat. A: Changes made with continuous current injections. The stimulus intensity was kept constant just below firing threshold. Traces in the third row (Vm) were recorded without current injection, the top two under depolarizing, the lower three under hyperpolarizing current. Dotted line in each rows indicates original baseline level. B: Responses evoked from another cell in the same slice. 1,2: Effects of -0.5 nanoA, 50 ms pulses: hyperpolarization retarded or blocked the spike initiation and enlarged the PSP component. Superimposed sweeps, MF stimulus constant. 4: Three intracellular responses to weaker volleys of varied intensity and 3: extracellular potential taken after pulling the pipette back from the cell. Distance between traces 4 and 3 corresponds to the membrane potential.

hyperpolarizing IPSP (Fig. 4.4.). In some cells quite low (0.2 Hz or less) rate of spontaneous irregular solitary action potentials as well as subthreshold PSPs were noted. Barely detectable AHP followed spontaneous spikes. Evoked postsynaptic action potentials were followed with larger hyperpolarization indicating presence of IPSP component.

A total of 17 cells impaled in the CA3 area of slices from irradiated rats were treated with KA. Of these 11 responded with strong bursting and 9 of these were impaled in slices cut from the temporal hippocampus. In 4 of these 11 cells KA induced spontaneous firing (solitary spikes) and subthreshold PSP activity was also noted. In one cell KA quickly depressed all activity and in 5 cells no effect of KA was detected during 5 min exposures. Five of these 6 cells were found in the slices cut from the septal part of the hippocampus. Some quickly reacting cells were exposed to KA for short periods only and intracellular recording continued until effects of the agonist were washed out. In addition, 8 cells impaled in irradiated slices were lost during KA application, but bursts were seen in 3 of them found in the temporal hippocampus. Although these cells were discarded from the analyzed group, data from them supported the assumption that a major portion of CA3 pyramidal cells impaled in the temporal, rather than in the septal hippocampus of irradiated rats could react with bursts to KA application.

Early effect of KA promoted spontaneous firing (Fig. 4.5. B), then bursting (Fig. 4.5.C), while the evoked responses remained unaltered. Large hyperpolarization, considered burst AHP followed each groups of 3-8 action potentials. Later the rate of bursting increased and several - instead of single - spikes occurred in responses to MF volleys (Fig. 4.5.D). In other cells bursts replaced solitary spikes in evoked responses before spontaneous burst were observed. Baseline shift to depolarizing direction was regularly noted (Figs 4.5. and 4.6.). During the stage of high rate of spontaneous bursting, baseline depolarization and depression of both the burst-AHPs and the evoked IPSPs were evident. Diminution of IPSP with depolarization was expected (Fig. 4.4.A) but AHP was presumed to grow with depolarization.

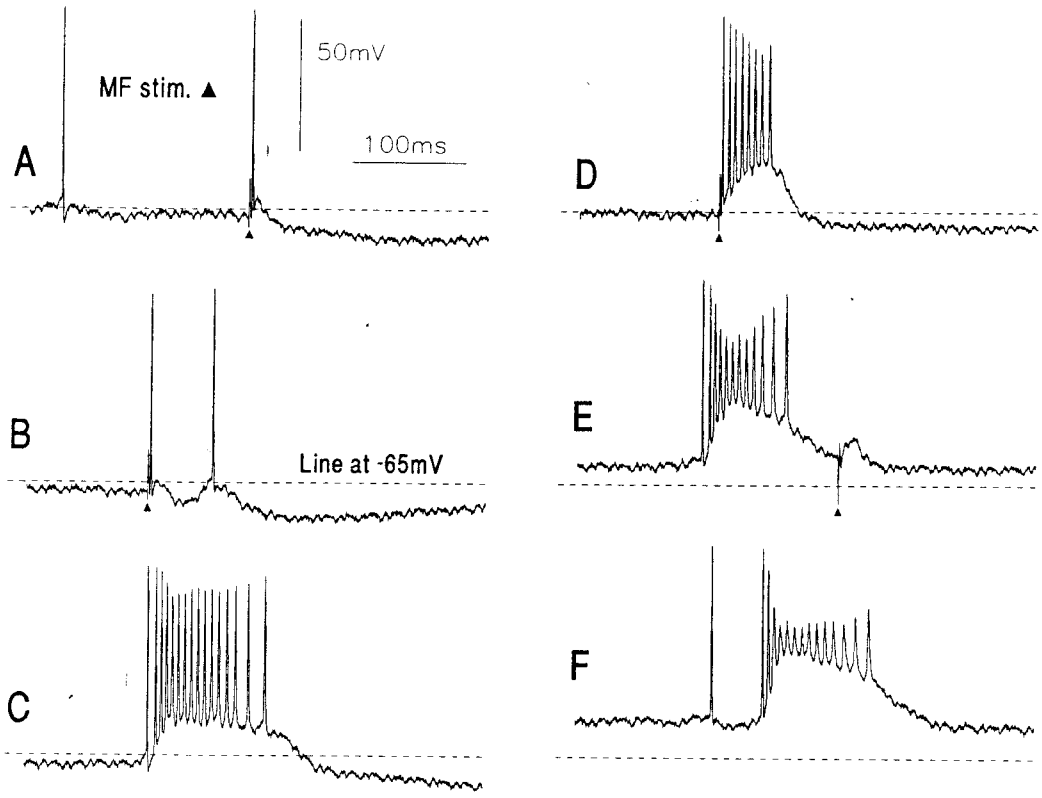


**FIGURE 4.5.** Selected frames from a tape-recorded period of intracellular recording before and after KA application (300 nM) Slice from the temporal half of the hippocampus of an irradiated rat. Dashed lines at -65 mV helps to compare waveforms. A: Before KA application, examples of single solitary spontaneous action potentials followed by small AHP and of MF evoked single discharges followed by large hyperpolarization. B: A spontaneous spike occurs during the evoked IPSP, a frame taken in the early period of KA application. C: Spontaneous burst during the second minute of KA inflow. D: During KA application MF volleys induces a burst of action potentials. E: The MF volley fails to discharge the cell after a spontaneous burst. Note the baseline depolarization and missing of evoked IPSP component. F: Later on the baseline was even more depolarized but bursting continued.

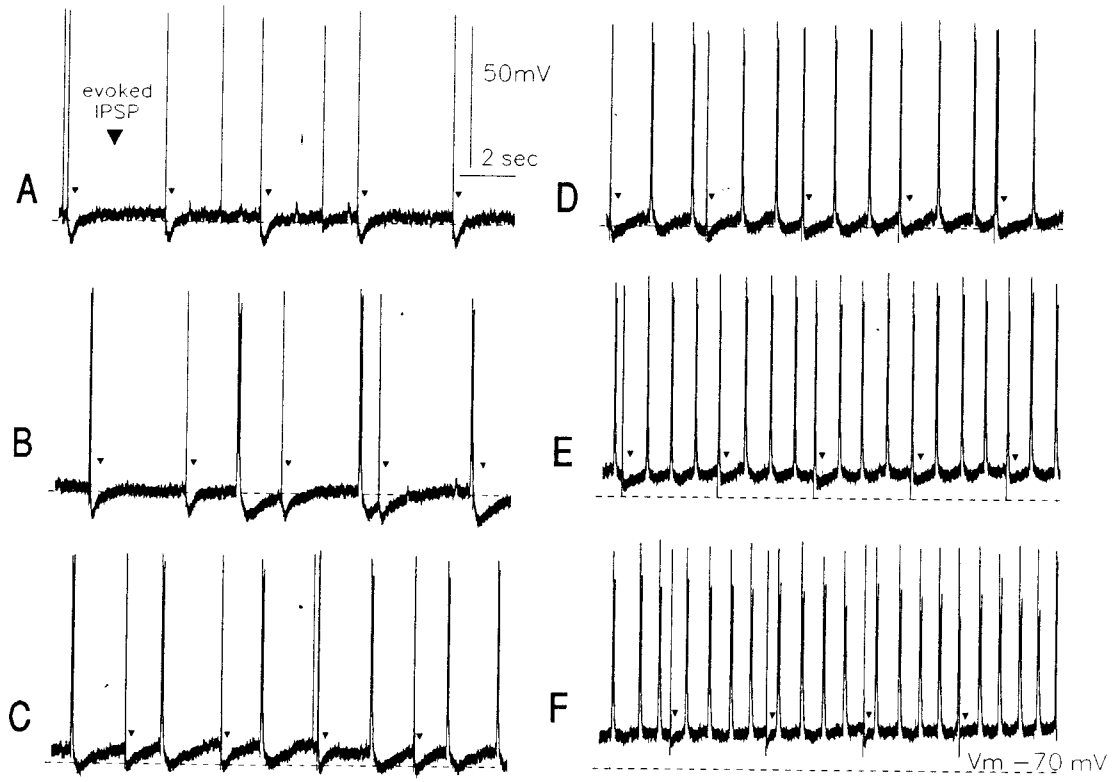


**FIGURE 4.6.** Progress of kainate-induced reaction in an irradiated CA3 pyramidal cell recorded in a slice cut from the temporal half of the hippocampus. A: In the sample taken before KA application there were 3 spontaneous solitary action potentials, and the MF evoked responses contained large IPSP components. B: At about 1 min after KA application (300 nA) there were a few spontaneous bursts which interacted with the evoked responses. Both the evoked IPSPs and the burst-AHPs were large. C, D, E: samples taken at 99, 125, and 154 sec after KA application, respectively. Frequency of spontaneous bursts increased, amplitude of both the evoked IPSPs and burst-APHs decreased, and the baseline depolarized progressively. F: At 3 min after KA application the membrane potential decreased further, spontaneous bursts come with high rate and no hyperpolarizing components followed either the spontaneous or the evoked firings. Dashed line marks the -70 mV membrane potential in each frames and the calibration in A refers for A-F.

Like in cases with extracellular recordings, KA had no effect on spontaneous activity in some ($n$ = 5) impaled cells. They were simply depolarized slightly in the first minute of KA inflow and during continued KA application either their membrane potential decreased further suggesting damage, or depression of evoked responses become obvious. Four of the five cells were found in slices from the septal hippocampus.

## DISCUSSION

The main findings of the here presented data is a suggestion of a quantitative relationship between magnitude of projection from the dentate gyrus and the degree of excitability of CA3 pyramidal cells by kainic acid. Our sample does not allow an estimation of likelihood of KA-induced bursting of CA3 pyramidal cells in irradiated slices but supports the view that in spite of strong reduction of their MF inputs, many pyramidal cells fire to volleys arriving in the residual MF and some remain able to generate spontaneous bursts to KA application.

Irradiation induced morphological changes was discussed in Chapter 2, and only some short comments are repeated here. Determination of density of granule cells was made in intracardially perfused animals, because this technique results better tissue preservation for histological purposes than the one used for processing tissue after electrophysiology.

Decrease of both direct cell counts and areas occupied by the somata of granule cells, as well as changes of MF bundle were uneven in individual animals, and the consistently larger septal than temporal damage can explain why KA promoted SRPA more often in slices cut from the temporal, than from the septal part of the hippocampus.

The quantitative data presented here suggest that if the irradiation destroys up to 50% of granule cells and a small number of cells in the hilus, the residual MF projection to CA3 area can maintain normal sensitivity of pyramidal cells to KA. On the other hand, about 70-80% reduction of granule cells prevents the CA3 pyramidal cells to react to KA application with epileptiform bursting. Such reduction was accompanied by a 30%

decrease of hilar cells. This assumption comes from lower probability of KA-induced bursts in the septal slices, where the granule cell loss approached 80%. The reduction of the MF bundle was parallel but not proportional with the loss of granule cells. In all cases the MF bundle was larger than expected from the degree of granule cell loss. This result suggests that remaining granule cells give rise to a larger projection field, probably due to a limited MF sprouting inside the hilar region and in stratum lucidum of CA3 area. Other factors may also be involved. Moser et al. (1993) discussed recently the different functional significance of the changing connectivity of cells along the septotemporal axis of the hippocampus and supported earlier assumptions (e.g. Nadel, 1968) by quantitative data.

Gaiarsa et al. (1994) showed that irradiation-induced MF loss did not significantly alter the responses of CA3 pyramidal cells to stimulation of commissural and associational fibers. Our data complete those observation with demonstrating that volleys in residual MF bundles induce EPSP-IPSP sequence and monosynaptic action potentials in virtually all CA3 cells studied with intracellular recording. They did not determine the limit of granule cell loss required to prevent KA-induced SRPA but noted that in 29% of the slices the KA remained effective. Since KA induced SRPA as well as burst firing can be demonstrated in some but not all irradiated rats, a likely reason of variability could be the ratio of lost and residual granule cell population. The limit may be between 50 and 80% because destruction of half of the granule cells does not prevent KA induced epileptiform activity, while it was missing if the granule cell loss reached 80%. Caution is however required to evaluate failures of detection of SRPA as indication that KA is unable to induce burst firing of CA3 cells in irradiated rats, because the extracellular discharges may remain small, the frequency low and toxic effect of KA (depression) may soon become dominant.

# Chapter 5.

# SEVERE SPATIAL NAVIGATION DEFICIT IN THE MORRIS WATER MAZE AFTER SINGLE HIGH DOSE OF NEONATAL X-RAY IRRADIATION IN THE RAT

## INTRODUCTION

As discussed in the General Introduction there is considerable evidence indicating that the rat hippocampal formation is critically involved in the neural representation of space. Spatial localization is seriously impaired after different kinds of hippocampal damage (Morris et al., 1982; Sutherland et al., 1983) and pyramidal cells in the hippocampus discharge selectively at specific locations of the environment (O'Keefe and Dostrovsky, 1971; Muller et al., 1987). Notwithstanding this information about the effects of global hippocampal lesions on spatial learning, the contribution of discrete subregions of the hippocampus is less well understood (Sutherland et al., 1983; Moser et al., 1993; Stubley-Weatherly et al., 1996). Studies using the Morris water maze have revealed important differences between selective lesions of the dorsal and ventral hippocampus (Moser et al., 1993), and the dorsal CA1 and ventral CA3 subregions (Stubley-Weatherly, 1996). Studies inducing different types of dentate gyrus lesions either with colchicine injection (Sutherland et al., 1983; McNaughton, 1989; Whishaw, 1987; Schuster et al., 1997), or by adrenalectomy (Armstrong et al., 1993; Conrad and Roy, 1993) yielded ambiguous results. Although it is well established that all three principal subfields of the hippocampus receive direct projections from the entorhinal cortex (Steward and Scoville, 1976; Witter et al., 1988; Yeckel et al., 1988), the dentate gyrus is considered to be the first stage of the classical "trisynaptic pathway" (Andersen et al., 1971; Lomo, 1971) as the dentate granule cells receive their major afferent input from the entorhinal cortex and relay the information coming through this pathway to the rest of the

hippocampus. What kind of behavioral consequences could be produced by removing the first stage of intrahippocampal information processing, by selective elimination of the granule cells of the dentate gyrus?

Does neonatal single dose of X-ray irradiation lead to serious behavioral deficits in adulthood, or is the early damage compensated during development?

In the present study the highest possible dose (9 Gy) of X-ray irradiation was applied on the first postnatal day to elicit a large loss of granule cells and a maximum navigation impairment.

## MATERIALS AND METHODS

### Animals

Thirty-two Long Evans hooded were used in this study.

### Apparatus and tracking system

The Morris water maze was a uniformly blue circular pool (2 m in diameter and 55 cm high) filled to a depth of 25 cm with water (20 °C). Rats could escape by climbing either on a visible platform in the *Cued Navigation Task*, or on a submerged invisible platform in the *Place Navigation Task*. The platform was a clear Plexiglas cylinder 11 cm in diameter, which stood 1 cm below the water surface in the middle of one of the four quadrants of the pool in the place task and was topped with a 3 cm thick dark disk in the cued task. The pool was located in a large room which was indirectly illuminated by several lamps allowing the rats to see numerous remote landmarks.

During each trial, an infrared light-emitting diode (LED) connected to a counterbalanced thin cable was attached to the animal's body with a rubber band. An infrared-sensitive television camera was mounted over the center of the pool and used for monitoring the LED movement. Every 100 ms, the computerized tracking system monitored and stored the position of the LED-indicated rat.

**Behavioral training**

A trial began by taking the animal from the waiting cage and placing it into the water facing the wall of the pool at one of the four arbitrarily designated points that marked north, east, south, and west (N, E, S, W). The tracking system was started at the time the animal was released. The maximum time the rat was allowed to swim was 60 s. The trial stopped either after this time had expired or after the animal had found the platform and remained on it for more than 1 s. When the rat failed to find the platform it was led to it. Climbing onto the platform was the only way of escaping from the water. The animal was always allowed to rest there for 15 s before it was returned to the waiting cage. The next trial was started approximately 15 s later. Each training day consisted of a two blocks, 8-trial session. After the last trial, the animal was towel dried and put into a cage under a heating lamp before being returned to the home cage.

**Data Analysis**

Overall treatment effects were assessed with either one- or two-way ANOVAs, and Scheffe's comparisons and Tukey's protected *t*-test were used in a post-hoc analyses to further evaluate significant effects. Student *t*-test for independent or paired values were used where appropriate. Results are presented as the mean ± SEM. Because latency and path length measures were highly correlated and yielded similar conclusions, only latency is reported.

# RESULTS

## Experiment 1: Invisible platform in light

Six naive irradiated and 6 naive control rats were trained in 10 daily sessions to escape to the underwater platform in the center of the South-West quadrant of the pool. The start positions were randomly distributed by the computer so that all four starting points were used in a block of four trials. Two blocks made one session (8 trials per session).

The control group rapidly learned to find the platform and reached on day 4 the asymptotic performance of 8 s which was not statistically different from the mean 6 s latency in the last 5 days of training (Fig. 5.1.). The irradiated rats swam around the wall of the tank, did not follow the experimenter's hand leading them to the platform after 60 s, and did not stay on the platform when they found it. Later, most of the irradiated rats learned that an escape platform is somewhere inside the pool and started to leave the wall and search it on a random path (Fig. 5.1.A). They could not navigate, however, averaging an escape latency of 50 s on day 5 and not improving in the last 5 days of training (Fig. 5.1.B). The two groups were significantly different already on day 1 ($t(10) = 2.9$, $P < 0.01$).

## Experiment 2: Visible platform

This task, corresponding to simple cue-directed locomotion can be learned by hippocampectomized rats but requires intact vision. The same rats and apparatus were used, but the location and form of the platform was changed. The dark gray platform (18 cm in diameter) stood about 1 cm above water surface in the center of the North-East quadrant of the pool. The animals were trained for 3 days.

The control group rapidly learned to escape to the new platform and reached the 5 s asymptote on day 2. Longer escape latency on day 1 ($t(5) = 6$, $P < 0.01$) was due to initial search in the previous location of the goal. The irradiated rats had an average latency of 40 s on day 1 and this did not change during the 3 days (Fig. 5.2.). They did not notice the visible platform even when swimming close to it, did not turn and climb upon it.

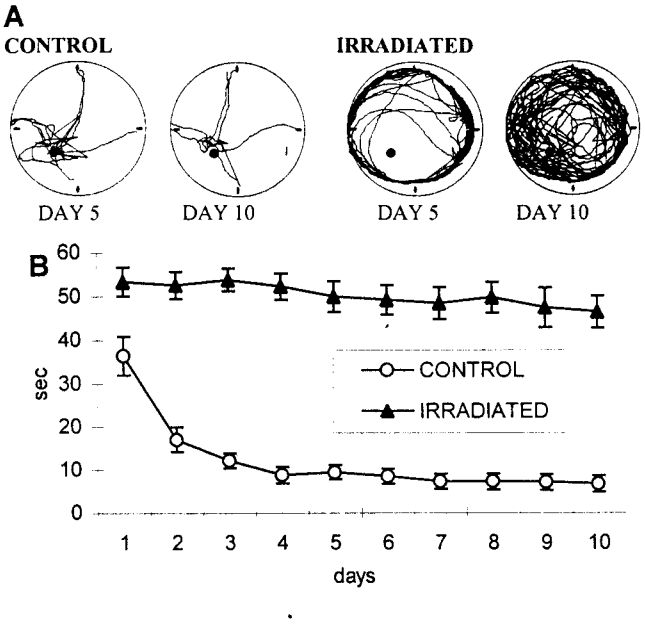


**FIGURE 5.1.** (A) Computer printouts of superimposed swimming trajectories of a control and an irradiated rat, trained in light, to find an invisible platform when started from any of the four cardinal points (north, east, south, west) at the circumference of the pool. Control rats headed towards the target, whereas the irradiated rats swam mostly near the wall of the pool (on day 5). By day 10 the irradiated rats covered the entire surface of the pool. (B) Latency to find the platform in irradiated and control rats. The performance of the control rats improved to the asymptote by day 4, whereas that of the irradiated rats remained almost unchanged, suggesting that irradiated animals are unable to learn the task.

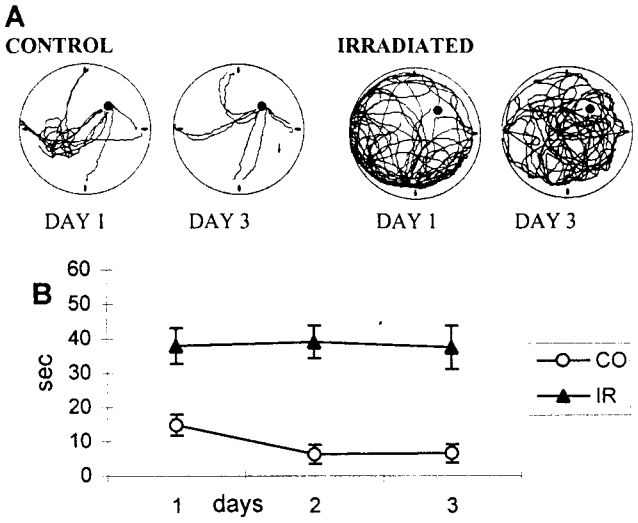


**FIGURE 5.2.** (A) Computer printouts of the superimposed swimming trajectories of a control and of an irradiated rat, trained in light, to find a visible platform when started from any of the four cardinal points (north, east, south, west) at the perimeter of the pool. The position of the platform was shifted from southwest to northeast. On the first day, the control rats swam initially to southwest, spending a few seconds there before approaching the visible platform in northeast. On day 3, they swam straight to the platform from all starting points. The irradiated rats covered the entire surface of the pool, never achieving a more compact and efficient form. (B) Latency to find the visible platform in control (CO) and irradiated (IR) rats. The control group reached asymptote of 5 sec on the second day. The irradiated rats had an average latency of 40 sec on day 1, and this did not change during the following two days.

The decrease in average latency from Exp. 1, probably was due to the larger diameter of the platform and increased possibility of chance detection. These results demonstrate that irradiation caused severe visual deficits interfering with navigational performance.

**Experiment 3: Navigation in complete darkness**

To decide whether the spatial navigation impairment of the irradiated animals found in Exp. 1 and 2, was caused by granule cell loss in the dentate gyrus or by impaired vision, new groups of naive control and irradiated rats were trained during 4 weeks in complete darkness under conditions of fixed start-fixed target geometry which were previously shown to be compatible with successful navigation (Moghaddam and Bures, 1996).

The procedure described in the Materials and Methods was followed using n=8 naive control and n=12 irradiated rats. The windows of the experimental room were carefully covered and the tracking system, that was located in an alcove in one corner, was separated by a black curtain in order to eliminate all sources of light and consequently any visual cues. Rats were trained in 28 consecutive daily sessions.

The control rats gradually learned to search for the platform in the inner part of the pool. After initial circling and attempts to climb the wall they started to spend more time in the inner part the pool and gradually oriented toward the target (Fig. 5.3.A). Their average escape latencies were 40 s in the first week (7 days per week), 24 s in the second, 17 s in the third and 13 s in the fourth week (Fig. 5.3.B).

The irradiated rats behaved similarly as those used in Exp. 1: they swam almost exclusively around at the wall (Fig. 5.3.A) and when the light was switched on, they did not follow the experimenter's hand leading them to the platform and did not stay on the platform when placed on it by hand. Later, they learned to rest on the platform but they still spent most of their 60 s circling around the wall of the pool in one direction. After intensive training some started to cut arcs from their swimming circles and occasional found the platform (Fig. 5.3.A). In general, the improvement of the irradiated rats was marginal and slow, but there were substantial differences

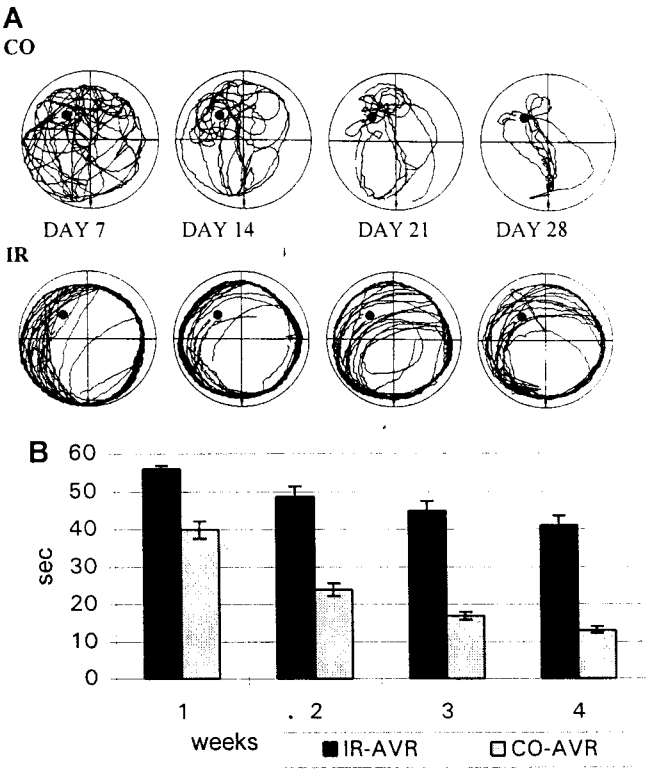


**FIGURE 5.3.** (A) Computer printouts of superimposed swimming trajectories of control (CO) and irradiated (IR) rats trained in darkness. The rats start at south, and the position of the platform at northwest is indicated by a black dot. The irradiated rats mostly swam close to the wall of the pool, and covered a crescent-shaped area around the platform, whereas the trajectories of the control rats contracted gradually to a compact and efficient form by day 28. (B) Latency to find the platform in the dark, under fixed start (south)-fixed goal (northwest) conditions, by the control (CO-AVR) and irradiated (IR-AVR) rats. The columns represent the mean (±S.E.M.) escape latency in 7-day blocks.

between individual rats. On some days, the mean escape latency of the best performing irradiated rat was shorter than the average escape latency of the control group. Nevertheless, the performance of the irradiated group was poor and their mean escape latency on the fourth week of training did not reach that of the controls on the first week (Fig. 5.3.B). A two-way ANOVA (groups X weeks, 2 X 4) with repeated measures on the last factor revealed significant main effects of groups, $F(1, 18) = 85.75$, $P < 0.0001$, and of weeks $F(3, 54) = 91.21$, $P < 0.0001$ as well as significant interaction $F(3, 54) = 8.93$, $P < 0.0001$. Scheffe's comparisons revealed significant differences between the control and irradiated groups within each of the four weeks ($P < 0.01$).

The results of Exp. 3 clearly suggest that the spatial navigation impairment found in Exp. 1 could not only be attributed to the visual deficit, because the irradiated rats also performed significantly worse than intact rats in total darkness.

**Experiment 4: Start-goal rotation in darkness**

The purpose of this experiment was to test the relative contributions of allocentric memory and egocentric memory to the poor spatial performance of the irradiated rats. A previous study (Moghaddam and Bures, 1996) showed, that navigation performance of overtrained control rats in total darkness is at least partly due to allocentric memory for the position of the goal with respect to acoustic beacons. To evaluate the possibility that irradiated rats used allocentric memory we exposed the irradiated rats to a start-goal position change. After a one-week break, we held a retraining phase for three days, using the same method of training, after which the start and goal positions were rotated by $90^{\circ}$ clockwise (from south-northwest to west-northeast). The effect of the start-goal rotation could be observed in the first 5-s trajectories. Although rotation should have no effect on egocentric navigation, the trajectories of the typical control rat shifted in the direction of the allocentric location of the previous goal (Fig. 5.4.A). On the next day the trajectories of the control rats were somewhat dispersed but were directed more toward the new target position. On the last

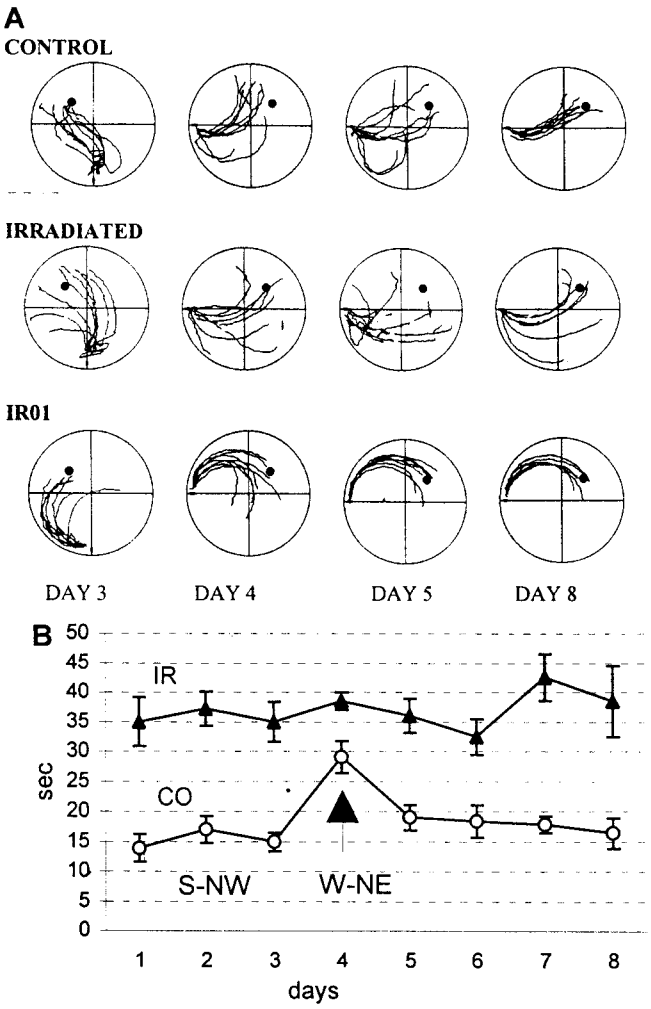


**FIGURE 5.4.** (A) Computer printouts of the eight superimposed swimming trajectories (first 5 sec of each trial) for a typical control rat, a typical irradiated rat, and the best (IR01) irradiated rat. Note that the control rat on the day of change (day 4) swam more toward the previous position of the platform. Their trajectories were somewhat dispersed on day 5, becoming more compact and efficient again by day 8. The dispersed trajectories of the typical irradiated rat were barely affected by the change in platform location on day 4, whereas the heading direction of the best-performing irradiated rat (IR01) was also largely unaffected by the change. (B) Average latency to find the platform on successive days of retraining before and after the platform location was changed to northwest-northeast on day 4 (indicated by arrow). Note that the latency of the control (CO) group almost doubled on day 4, but that no noticeable increase was observed in the irradiated (IR) group.

day of training they assumed a nice compact appearance again (Fig. 5.4.A). On the other hand, the dispersed trajectories of a typical irradiated rat were hardly influenced by the change (Fig. 5.4.A). Even the heading direction of IR01, the best performing irradiated rat, proved to be quite stable. This suggests that its first 5-s trajectories were generated by egocentric mechanisms (Fig. 5.4.A).

During the 3 days of retraining the average escape latencies of the control rats were around 15 s, while the irradiated animals had an average escape latency of 35 s. On the fourth day (the day of change), the mean escape latency of the control animals was almost doubled, whereas that of the irradiated rats remained unchanged (Fig. 5.4.B). The last day of south-northwest training was compared with the first 2 days of west-north-east training using a two-way ANOVA (groups X conditions, 2 X 3) with repeated measures on the last factor which yielded significant main effects of groups ($F(1, 14) = 38.70$, $P < 0.0001$) and of conditions ($F(2, 28) = 6.52$, $P < 0.01$.), as well as significant interaction ($F(2,28) = 3.70$, $P < 0.05$). Tukey's protected $t$ tests showed significant difference between the third and the fourth day's latencies for the control rats ($P < 0.01$) but not for the irradiated rats.

## DISCUSSION

Experiments of this chapter demonstrates that the acquisition of place navigation in the Morris water maze is severely disrupted in adult rats whose brains were exposed shortly after birth to a single high dose of X-ray irradiation. It is conceivable that this deficit can be accounted for by the loss of 60 to 80 % of granule cells in the dentate gyrus. Such conclusion must be accepted with caution, however, because irradiation may also damage other brain circuits critical for place navigation.

The results of Exp. 1 indicated that irradiated rats are not able to follow the experimenter's hand leading to the goal. The possibility that their vision is severely impaired was confirmed in Exp. 2. The irradiated rats were unable to find a clearly visible escape platform, which was easily located by the control rats. Because such cue-directed locomotion is not disrupted by hippocampectomy (Jarrard, 1983), the failure of irradiated rats in this task cannot be ascribed to dentate gyrus lesion but rather to poor vision. Visual loss caused by neonatal irradiation of brain was reported by Stewart-Amidei (Steward-Amidei, 1995). Histological examination of the retinas of irradiated rats showed significant loss of ganglion cells as compared with controls.

To eliminate the effect of irradiation-induced visual deficit on navigation, new groups of control and irradiated rats used in Exp. 3 learned fixed start - fixed target navigation task in darkness. Acquisition was significantly slower in the irradiated rats than in the control animals. The latter group replicated the results obtained in intact rats (Moghaddam and Bures, 1996), which reached an escape latency of 16 sec after 4 weeks of training. Although the role of the hippocampus in path integration is not fully understood, the results of Exp. 3 suggest that the failure of irradiated rats to master the fixed start - fixed goal navigation task may be due to the granule cell loss and to the ensuing modifications of hippocampal circuitry. The latter factor may account for the differential effect of various types of dentate gyrus lesions on place navigation (Sutherland, 1983; Conrad and

Roy, 1993; McNaughton et al., 1989) and on place cell activity (McNaughton et al., 1989).

The fixed start - fixed goal navigation task in darkness could be used whenever navigation performance might be compromised by possible visual deficits (Morris., 1984). It must be pointed out, however, that this task does not completely eliminate allocentric orientation. Intact rats can use not only egocentric route memory but also allocentric memory for non-visual extra-maze cues, e.g. acoustic beacons (Moghaddam and Bures, 1996). The relatively short escape latency in the control group of Exp. 3 is due to the combined effect of egocentric and allocentric orientation; the relative contributions of these components to the performance of control and irradiated rats was assessed in Exp. 4. After simultaneous rotation of the start and goal positions, egocentric solution of the task remains correct, whereas allocentric orientation guides the animal incorrectly. The conflict between these two components caused the almost two-fold increase of escape latencies in the control group but no comparable change was seen in the irradiated rats. The trajectories produced during the first 5-s of each trial suggest that the irradiated rats solved the task using egocentric navigation only, which accounts for the slower acquisition rate. Purely egocentric navigation in the fixed target - fixed goal situation has been studied by Save and Moghaddam (Save and Moghaddam, 1996) by preventing allocentric orientation with daily changes of start and goal positions. After 24 days of training under these conditions the mean escape latency was 27 s, i.e. almost twice as long as seen in the present control rats, who were using allocentrically supported egocentric navigation. The performance of irradiated rats is worse, however, than would correspond to the absence of allocentric orientation. Therefore it seems likely, that irradiation also has interfered with the neural circuits supporting egocentric orientation, perhaps including cortical regions participating in the processing of vestibular and kinesthetic signals implementing path integration.

Histological examination showed that the irradiated rats have in addition to the loss of dentate granule cells a thinner corpus callosum and

thinner cortex above the hippocampus. The latter change was due to the loss of granule cells in layer III and IV and to a reduced number of glia cells in all cortical layers. The region affected corresponds to the associative parietal cortex; the bilateral lesions in this area impair performance in various spatial tasks requiring allocentric coding of space (Kolb et al., 1983; Kolb and Walkey, 1987; DiMattia and Kesner, 1988; Save et al., 1992) and even in a task based on purely egocentric coding of space (Save and Moghaddam, 1996). On the other hand, the thinner cortex above hippocampus is not comparable with complete bilateral removal of associative posterior cortex. Cortical tissue overlying the hippocampus is routinely damaged in behavioral studies using aspiration lesions of the hippocampus. Sham operated controls in such studies show that similar cortical lesions do not significantly deteriorate spatial learning (Moser et al., 1993).

In conclusion, an intact dentate gyrus is critical for hippocampal function in space navigation. Prevention of granule cell formation by neonatal X-ray irradiation is as effective in disrupting navigation as is removal of those cells in adulthood, suggesting that plastic changes of the hippocampal circuits can not compensate for the loss of granule cells.

# Chapter 6.

# LATERALIZED FASCIA DENTATA LESION AND BLOCKADE OF ONE HIPPOCAMPUS: EFFECT ON SPATIAL MEMORY IN RATS

## INTRODUCTION

Interhemispheric transfer (IHT) of lateralized engrams demonstrates that what is learned with one side of the brain can be not only retrieved and used by the other side, but even copied into the naive side. Unilateral functional blockade by tetrodotoxin (TTX) or lidocaine injection into fimbria-fornix and dorsal hippocampus (Fenton and Bures, 1993; 1994) makes it possible to form lateralized spatial memories which can be rapidly transferred from the trained to the naive hippocampus after the latter recovers from the TTX inactivation (Fenton et al., 1995). It was suggested that the transfer is mediated by interhippocampal commissural pathways activated when the task is performed with intact brain.

As discussed in the previous chapter neonatal X-ray irradiation induced degranulation produce severe spatial navigation deficit in adult rats tested in the Morris water maze.

Lateralized irradiation destroying the FD only in one hemisphere makes it possible to compare place navigation during unilateral functional ablation of the irradiated or of the intact hippocampus.

We asked whether the absence of the spatial learning deficit in the unilaterally irradiated rats can be due not only to the normal function of the intact hippocampus but also to spatial learning supported in the irradiated hippocampus by the commissurallly mediated input from the intact hemisphere.

# MATERIALS AND METHODS

## Animals and X-ray irradiation

Seven male rats from the Long Evans strain was used in this study. The irradiation procedure was described in Chapter 2., but the lead-coated shield used in these experiments was different. It had a smaller half-circle opening above the dorsal hippocampus on the right side, which allowed making even smaller lesions.

## Surgery

To permit hippocampal TTX inactivation, the adult rats, at the age of 90-110 days, were anaesthetized with pentobarbital (50 mg/kg, i.p.) and two stainless steel guide cannulae (0.4-mm inner diameter) were bilaterally implanted into their skulls (3 mm antero-posterior [AP] on the non-irradiated side and 4.5 mm AP on the irradiated side respectively, and ±2.5 lateral [L] to bregma in both sides). The cannulae and three anchoring assemblies were cemented both together and to the bone with dental acrylate. The 10-mm-long guide cannulae extended 2 mm dorsoventrally (DV) into the brain: the tip was aimed to rest at the ventral surface of the corpus callosum, above the dorsal hippocampus, according to the atlas of Fifkova and Marsala (1967).

## Injection procedure

After at least one week's recovery, at each injection day, 40 to 60 min. prior to training, the implanted rats were restrained and unilaterally injected with 10 ng of TTX dissolved in 1 µl of physiological saline. A stainless steel injection needle (0.3-mm outer diameter) was inserted into the guide cannula to protrude 1.5 mm beyond its tip so that the injection position was in the dorsal hippocampus at AP = 3, L = ± 2.5, and DV = 3.5 Fifkova and Marsala (1967). The TTX solution was gradually delivered over the course of 1 min. via a 10 µl Hamilton syringe attached with polyethylene

tubing to the injection needle. Ninety seconds after the injection, the needle was slowly removed and the rat was returned to its home cage.

**Apparatus and tracking system**

The apparatus and tracking system was previously described in Chapter 5.

**Behavioral training**

The behavioral training was previously described in Chapter 5.

*Probe Trial:* To gain more data, probe trials were held in the end of the training days. It required each rat to swim in the pool for 60 seconds in absence of the platform. Presumably, if the rat has learned the precise location of the platform in the maze, it would spend the most time in the target quadrant, where the platform was formerly located

**Histology and Characterization of the Inactivation Procedure**

Proper interpretation of the results requires an assessment of the functional ablation technique, particularly the spatial extent of the inactivation and its duration. Figure 6.1. shows the track left by the injection assembly. The injections were always aimed within 0.5 mm of the intended target. There was usually evidence of some damage along the track of the injection cannule.

TTX is a powerful and highly specific blocker of the voltage-dependent $Na^+$ channels that mediate both impulse conduction and synaptic activity. Thus TTX's effect on neural tissue is global. Intracranial administration of TTX for functional ablation has been used in several behavioral studies (e.g. Ivanova and Bures 1990, Bermudez-Rattoni et al. 1991, Fenton and Bures 1993). Zhuravin and Bures (1991) showed that the spatial extent and duration of intracerebrally injected TTX can be characterized as diffusion from an instantaneous point source. Using the diffusion constant for TTX (Zhuravin and Bures 1991) and the equations describing diffusion from an instantaneous point source (Curtis 1964),

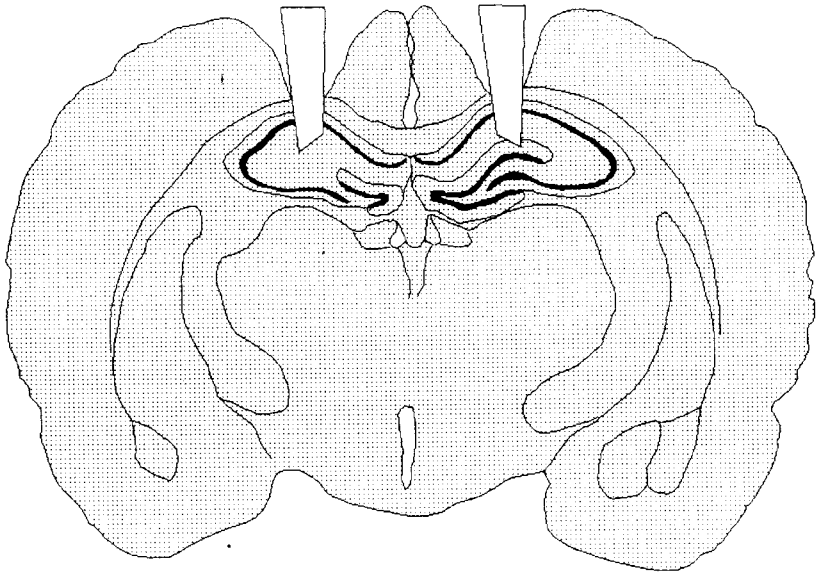

**FIGURE 6.1.** Neurolucida drawing of a representative coronal section showing the effect of unilateral irradiation and the injection sites. In the irradiated hemisphere, the dorsal blade of the dentate gyrus is greatly reduced, whereas the ventral blade is almost completely missing. The idealized drawing of the injection needle and the damage along the injection track indicates that the injections were in the dorsal hippocampus.

Zhuravin and Bures calculated that the volume of the effective TTX blockade at the time of training approximated that of a sphere with a diameter of 1.4 mm. Though the dynamic, the blockade should have lasted several hours (Cahill et al. 1987, Zhuravin and Bures 1991). These injections thus inactivated virtually all of the dorsal hippocampus extending to the fimbria fornix and thereby also deprived the hippocampal system of the cholinergic septal innervation responsible for the hippocampal theta rhythm (Buzsaki et al. 1983). Thus, the functional lesion elicited by TTX can be expected to dramatically compromise the functional integrity of the hippocampal system.

**Data analysis**

Similar statistical methods were used as in Chapter 5.

## RESULTS

We assumed that the spatial learning deficit caused by bilateral fascia dentata destruction will be absent during examination of the unilaterally irradiated rats because one intact hemisphere can support place learning. In addition, after excessive pretraining, the memory traces implementing place navigation in the Morris water maze which are presumably formed in the intact hippocampus can perhaps be transferred into the irradiated hippocampus by transcommissural information flow. If this happens, the presence of both memory traces will be manifested by equal retrieval of the overlearned task, tested during functional ablation of either hippocampus.

The aim of this experiment was (a) to examine the spatial learning ability of the unilaterally irradiated rats (b) to test the retrieval of an overlearned place navigation task during functional ablation of the irradiated or of the non-irradiated hippocampus, (c) to verify the possibility that the missing FD input of the irradiated hippocampus can be replaced by commissural input from the intact hippocampus.

The unilaterally irradiated rats were first pretrained to navigate to the hidden escape platform and retrieval of this task was then tested during unilateral functional inactivation either of the control or of the irradiated hippocampus.

During the 6-day long pretraining phase all rats were trained in 12 daily trials to escape from four starting points to an underwater platform hidden in the southeast quadrant of the pool. The purpose of this phase was to improve the animals performance to the truly asymptotic level of goal-directed navigation. Retrieval was tested during the four subsequent days: on days 7 and 9, unilateral TTX injections were made into the intact and irradiated hippocampus, respectively. No TTX was applied before retrieval testing on days 8 and 10 in order to demonstrate the reversibility of the preceding TTX treatment. Learning capability of the irradiated and intact hippocampus was examined by repeating the same sequence of tests on days 11 to 14. In addition, immediately following the last trial on days 6, 7 and 9 all animals were started from the North and given a 60-s probe trial with the escape platform removed.

**Pretraining phase (day 1 -6)**

All rats improved gradually in their ability to find the hidden platform and after 4 days of training reached the asymptotic level of performance (Fig. 6.2.). The average escape latency was 6.5 s on the last day of pretraining. One-way ANOVA of the average latencies of daily blocks revealed a highly significant effect of days [$F(5,30)= 85.55$, $P < 0.0001$] indicating fast learning. Tukey's *post hoc* comparison showed no significant differences ($P > 0.05$) among the final 3 days of pretraining. These data demonstrate that unilaterally irradiated rats can master the task as well as control animals, if they are allowed to use both hemispheres.

**First retrieval tests (day 7 - 10)**

The first injection of TTX into the non-irradiated hippocampus (1st TTX - CO) severely impaired the rats' performance (Figure 6.2.). Most rats

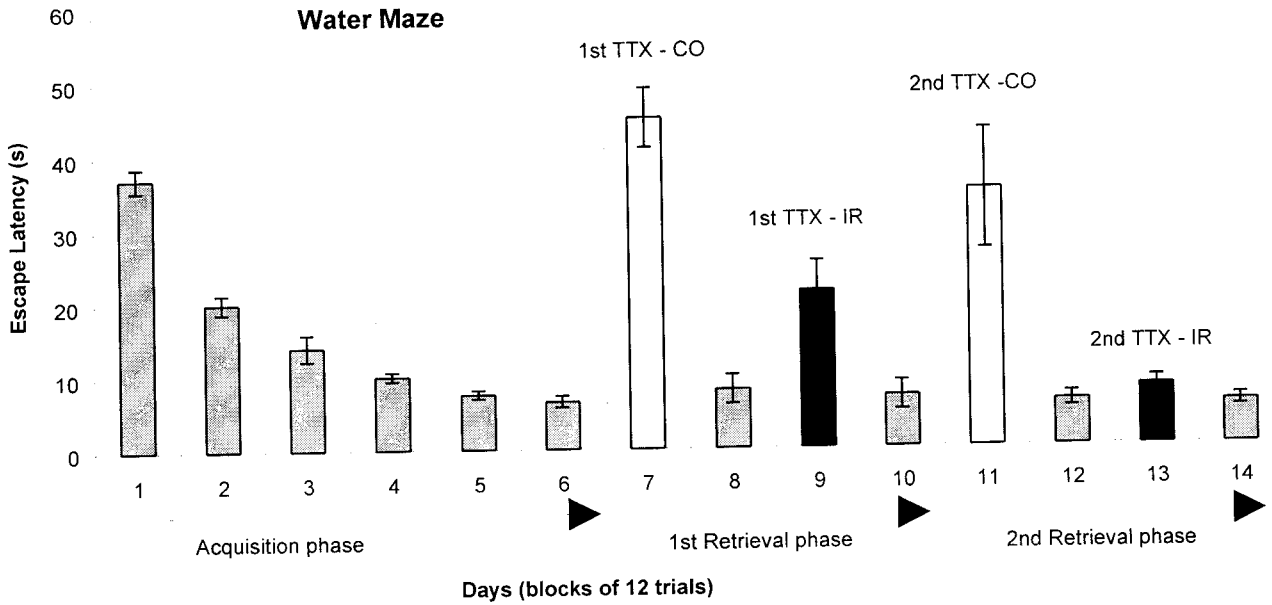


**FIGURE 6.2.** Experiment 2: Left side: acquisition in unilaterally irradiated rats without functional ablation. Right side: retrieval of place navigation during functional inactivation either of the intact (TTX - CO) or of the irradiated (TTX - IR) hippocampus, separated by training days without injection (abscissa). Ordinate: mean escape latencies (±SEM). Abscissa: days of training.

just swam along the wall and only a few managed to swim into the pool and find the platform by chance. The average escape latency on this day (day 7) was 45 s. The first injection of TTX into the irradiated hippocampus (1st TTX - IR) caused a less severe navigation impairement. All rats searched in the target quadrant and eventually found the platform after an average 21-s escape latency (day 9). One-way ANOVA with repeated measures comparing the average latencies of the last pretrainig day (day 6) with the first TTX - CO day (day 7) and TTX - IR (day 9) as well with the second TTX - CO day (day 11) and TTX - IR (day 13) revealed a significant effect of the experimental conditions [$F(4,24) = 14.41$, $P < 0.0001$]. Newman-Keuls multiple comparisons showed significant differences between days 6 and 7 ($P < 0.01$), 6 and 9 ($P < 0.05$) as well as 7 and 9 ($P < 0.01$).

Figure 6.3. shows the results of the probe trials performed at the end of pretraining (day 6), on the first TTX-CO day (day 7) and on the first TTX-IR day (day 9). The animals had a significant preference for the goal quadrant ($P < 0.01$) on the last day of pretraining and on the first TTX-IR day, but not on the first TTX-CO day ($P > 0.05$). Rats navigating with their irradiated hippocampus did not remember the target location and spent equal amount of time in each quadrant.

**Second retrieval tests (day 11 - 14)**

During the second functional blockade of the intact hippocampus by TTX (Fig. 6.2.) average escape latency decreased by 10 s, but Newman-Keuls test indicated that this difference is not significant. Though some rats improved to less than 20-s average escape latency on the second TTX-CO day (day 11), other rats were still circling along the wall of the tank. On the other hand, TTX injection into the irradiated hippocampus caused no impairement during the second retrieval test (second TTX-IR) and rats reached an average escape latency of 8.2-s on that day. The Neuman-Keuls test revealed no significant difference between the second TTX-IR day and the last day of pretraining.

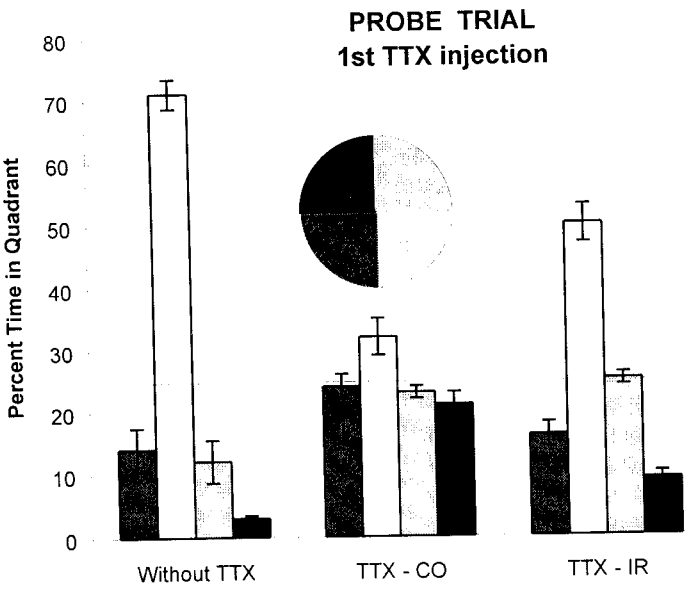


**FIGURE 6.3**. Results of the probe trials at the end of the last day of pretraining (without TTX) and at the end of those days when TTX was injected for the first time either into the intact (TTX - CO) or into the irradiated (TTX - IR) hippocampus. Ordinate: Mean percentage of time ( ± SEM) spent in the four quadrants.

## DISCUSSION

The behavioral data indicate that the unilaterally irradiated rats were able to acquire and retrieve place navigation in the Morris water maze with the intact brain as efficiently as non-irradiated rats with similarly implanted cannulae aimed at the hippocampus (Francis Turner et al. 1997). Retrieval tests performed during functional ablation of the irradiated hippocampus increased escape latency from 5 s to 21 s during the first and to 8 s during the second TTX inactivation, i.e. to values closely analogous to those reported after unilateral TTX injection into the hippocampus of similarly pretrained nonirradiated rats (17 s and 8 s, Fenton and Bures, 1993) which displayed, however, similar impairment caused by blockade of either hippocampus. This is in sharp contrast with the strikingly asymmetric effect of the TTX injection in the irradiated rats. The escape latencies were twice longer during first TTX blockade of the nonirradiated than of the irradiated hippocampus and this ratio increased to four times during the second TTX injection.

The initial weak impairment of place navigation elicited by the first inactivation of the irradiated hippocampus suggests that it may contribute in spite of the damage to the overall performance, e.g. by serving as an auxiliary output available through commissural pathways to the contralateral hippocampus with intact entorhinal input (Olton et al., 1982). Sudden elimination of this additional output probably participating in the procedural aspects of the task may account for the initial deterioration which is, however, rapidly compensated so that already the second blockade does not elicit a significant impairment.

The efficient compensation of the FD lesion is perhaps due to the fact that the lateralized irradiation was applied immediately after birth and the developing brain had ample opportunity to optimize the available connections of the intact hippocampus with the contralateral hemisphere. The contribution of the neocortex ipsilateral to the lesioned hippocampus could be tested by comparing the place navigation impairment caused by

functional blockade of similar cortical areas in the intact and lesioned hemisphere.

The failure of the place navigation engrams acquired by the intact hippocampus to spread into the lesioned hippocampus can be partly due to the limited capability of the latter to process ipsilateral entorhinal input. As shown by Fenton and Bures (1994) effective interhippocampal transfer does not occur spontaneously but only after several transfer trials have been performed with both hemispheres intact, i.e. requires convergence of the relevant entorhinal and comissural inputs to the naive hippocampus. Hippocampus lacking the FD input cannot profit from the commissural connections with the trained hippocampus performing the place navigation task, because the commissural signals are not supported by the corresponding entorhinal input. The present study does not answer the question, however, whether FD is necessary for the commissural retrieval of information which has been received by the lesioned hippocampus before FD elimination.

# Chapter 7.

## SUMMARY OF THE MAIN FINDINGS

The purpose of the present work was to describe the morphological and functional consequences of the partial degranulation of the hippocampus in newborn rats. We examined the triggering effect of removing the granule cells at three levels: *a*, structure of the organ (anatomical description of the lesion effect); *b*, cellular functioning (electrophysiology); *c*, complex behavior (spatial learning of the adult rats).

### Anatomy of the lesioned hippocampus

Systematic cell counts demonstrated a significant decrease in hilar cell number after irradiation. Immunostaining and histochemistry revealed that the number of both GABAergic and non-GABAergic neurons is reduced.

Our finding on irradiation-induced decrease of interneurons is a new discovery which accompanies previously reported histological damages.

Elimination of many granule cells and part of the interneurons disrupts the anatomical integrity and presumably the function of the most closely related hilus and CA3 area but perhaps the entire hippocampus. To our surprise, however, functional consequences were not spectacular.

### Electrophysiology of irradiated CA3 pyramidal cells

Consequences of major (50-80%) deafferentation of the CA3 pyramidal cells are difficult to recognize. Intracellular recordings combined with biocytin labeling in slice preparations revealed EPSPs of 2-5 ms latency, up to 19 mV amplitude, half-width of 5-20 ms, inducing monosynaptic discharges. Injected current affected the evoked PSPs: peak EPSP increased with hyperpolarizing current and differential reversal of early and late IPSPs were demonstrated. The size of PSP responses contrasts substantial reduction of the thorny excrescenses and spines.

KA induces epileptiform activity in the CA3 pyramidal cells of neonatally X-ray irradiated hippocampus. Partial removal of MF input reduces, but does not prevent, KA induced hyperexcitability of these cells. Important role a quantitative relationship between the size of the remaining MF bundle and the KA sensitivity of CA3 pyramidal cells is suggested, because removal of 80% of granule cells reduced hyperexcitability, whereas effect of 50% loss of granule cells could not be detected.

**Behavioral consequences of the neonatal insult: spatial learning abilities of unilaterally and bilaterally irradiated rats in the Morris water maze**

A single high dose of bilateral X-ray irradiation applied on the first postnatal day induce severe spatial navigation deficit in adult rats.

Unilaterally irradiated rats were able to acquire and retrieve place navigation with the intact side of their brain as efficiently as non-irradiated rats. Functional ablation either of the intact or of the irradiated hippocampus revealed strikingly asymmetric contribution of the hemisphere to the performance. Whereas the place navigation was severely impaired during blockade of the non-irradiated hippocampus, it was much less disturbed when the lesioned hippocampus was blocked. The inability of the FD lesioned hippocampus to process ipsilateral entorhinal input can also account for the failure of interhippocampal transfer which requires convergence of the relevant entorhinal and commissural inputs to the naive hippocampus.

## Chapter 8.

# REFERENCES

Acsády L, Kamondi A, Sik A, Freund T, Buzsáki G (1998) GABAergic cells are the major postsynaptic targets of mossy fibers in the rat hippocampus. J Neurosci 18:3386-3403.

Altman J, Anderson WJ, Wright KA (1969) Exp Neurol 24:196-216.

Altman J, Das GD (1965) Autoradiographic and histological evidence of postnatal hippocampal neurogenesis in rats. J Comp Neurol 124:319-335.

Altman J, Bayer S (1965) Migration and distribution of two populations of hippocampal granule cell precursors during the perinatal and postnatal periods. J Comp Neurol 301:365-381.

Andersen P, Bliss TVP, Skrede KK (1971) Lamellar organization of the hippocampal excitatory pathways. Exp Brain Res 13:222-238.

Amaral DG (1978) A Golgi study of cell types in the hilar region of the hippocampus in the rat. J Comp Neurol 182:851-914.

Armstrong JN, McIntyre DC, Neubort S, Sloviter RS (1993) Learning and memory after adrenelectomy-induced hippocampal dentate granule cell degeneration in the rat. Hippocampus 3:359-371.

Bayer SA (1980) Development of the hippocampal region of the rat. I. Neurogenesis examined with 3H-thymidine autoradiography. J Comp Neurol 190:87-114.

Bayer SA, Brunner RL, Hine R, Altman J (1973) Nature New Biol. 242: 222-224.

Bayer SA, Altman J (1975) Radiation-induced interference with postnatal hippocampal cytogenesis in rats and its long-term effects on the acquisitions of neurons and glia. J Comp Neurol 163:1-20.

Ben-Ari Y (1985) Limbic seizures and brain damage produced by kainic acid: Mechanisms and relevance to human temporal lobe epilepsy. Neuroscience 14:375-403.

Ben-Ari Y, Gho M (1988) Long-lasting modification of the synaptic properties of rat CA3 hippocampal neurones induced by kainic acid. J Physiol 404:365-384.

Benedikz E, Casaccia-Bonnefil P, Stelzer A, Bergold PJ (1993) Hyperexcitability and cell loss in kainate-treated hippocampal slice cultures. Neuroreport 5:90-92.

Bermudez-Rattoni F, Introini-Collison IB, McGaugh JL (1991) Reversible inactivation of the insular cortex by tetrodotoxin produces retrograde and anterograde amnesia for inhibitory avoidance and spatial learning. Proc Natl Acad Sci 88: 5379-5382.

Blackstad TW (1956) Comissural connections of the hippocampal region in the rat with special reference to their mode of termination. J Comp Neurol 105:417-538.

Bliss TVP, Collingridge GL (1993) A synaptic model of memory: long-term potentiation in the hippocampus. Nature 361:31-39.

Bliss TVP, Lomo T (1973) Long-lasting potentiation of synaptic transmission in the dentate area of the anaesthetised rabbit following stimulation of the perforant path. J Physiol (Lond.) 232:331-56.

Buckmaster PS, Kunkel DD, Robbins RJ, Schwartzkroin PA (1994) Somatostatin-immunoreactivity in the hippocampus of mouse, rat, guinea pig, and rabbit. Hippocampus 4:167-180.

Buzsáki G, Leung LS, Vanderwolf CH (1983) Cellular bases of hippocampal EEG in the behaving rat. Brain Res Rev 6:139-171.

Buzsaki G (1989) Two-stage model of memory trace formation: a role for "noisy" brain states. Neuroscience 31(3): 551-70.

Cahill L, Coopersmith RM, McGaugh LM (1987) Local injection of tetrodotoxin decreases metabolic activity in discrete brain regions: A 2-deoxyglucose autoradiography analysis. Society for Neuroscience Abstracts 13:1414.

Caronna JJ (1979) Diagnosis, prognosis, and treatment of hypoxic coma. In Fahn, JN Davis and LP Rowland (Eds) Advances in Neurology Vol. 26 (pp 1-16), Raven Press, New York

Chicurel ME, Harris KM (1992) Three-Dimensional analysis of the structure and composition of CA3 branched dendritic spines and their synaptic relationships with mossy fiber boutons in the rat hippocampus. J Comp Neurology 325:169-182.

Claiborne BJ, Amaral DG, Cowan WM (1990) Quantitative, three-dimensional analysis of granule cell dendrites in the rat dentate gyrus. J Comp Neurol 302:206-219.

Cobb SR, Halasy K, Vida I, Nyiri G, Tamás G, Buhl EH, Somogyi P (1997) Synaptic effects of identified interneurons innervating both

interneurons and pyramidal cells in the rat hippocampus. Neuroscience 79:629-648.

Conrad CD, Roy DJ (1993) Selective loss of hippocampal granule cells following adrenalectomy: implications for spatial memory. J Neurosci 13: 2582-2590.

Cohen NJ, Eichenbaum H (1991) The theory that wouldn't die: a critical look at the spatial mapping theory of hippocampal function. Hippocampus 1(3): 265-8.

Crespo D, Stanfield BB, Cowan WM (1986) Evidence that late-generated cells do not simply replace earlier formed neurons in the rat dentate gyrus. Exp Brain Res 62:541-548.

Cummings JL, Tomiyasu U, Read S, Benson DF (1984) Amnesia with hippocampal lesions after cardiopulmonary arrest. Neurology 34(5): 679-81.

Curtis DR (1964) Microelectrophoresis. In WL Nastuk (Ed) Physical techniques in biological research: Vol. 5. Electrophysiological methods. Part A (pp 144-192) San Diego, CA: Academic Press

Czéh B, Seress L, Houser L (1997) Number and distribution of $GAD_{65}$ mRNA-containing neurons in the rat hippocampal formation. (Abstract) 4th Congress of Hungarian Neuroscience Association, Neurobiology 5 (1)

Danscher G, Zimmer J (1978) An improved Timm sulphide silver method for light an electron microscopic localization of heavy metals in biological tissues. Histochemistry 55:27-40.

Dessi F, Represa A, Ben-Ari Y (1991) Effects of neonatal $\gamma$ - ray irradiation on rat hippocampus: Development of excitatory amino acid binding sites. Neuroscience 42:151-157.

DiMattia BD, Kesner RP (1988) Spatial cognitive maps: differential role of parietal cortex and hippocampal formation. Behav Neurosci 102(4): 471-80.

Dun NJ, Dun SL, Wong RKS, Förstermann U (1994) Colocalization of nitric oxide synthase and somatostatin immunoreactivity in the rat dentate hilar neurons. Proc Natl Acad Sci USA 91:2955-2959.

Fenton AA, Bures J (1993) Place navigation in rats with unilateral tetrodotoxin inactivation of the dorsal hippocampus: place but not procedural learning can be lateralized to one hippocampus. Behav Neurosci 107(4):552-64.

Fenton AA, Bures J (1994) Interhippocampal transfer of place navigation monocularly acquired by rats during unilateral functional ablation of the dorsal hippocampus and visual cortex with lidocaine. Neuroscience 58(3):81-91.

Fenton AA, Arolfo MP, Nerad L, Bures-J (1995) Interhippocampal synthesis of lateralized place navigation engrams. Hippocampus 5(1):16-24.

Fifkova E, Marsala J (1967) Stereotaxic atlases for the cat, rabbit and rat. In: Bures J, Petran M & Zachar J eds. Electrophysiological methods in biological research (3rd ed.) Prague, Czechoslovakia: Academia and San Diego: Academic Press, pp 653-731.

Fitch JM, Jaruska JM, Washington LW (1989) The dendritic morphology of pyramidal neurons in the rat hippocampal CA3 area. I. Cell types. Brain Res 479:105-114.

Francis Turner L, Liu Z, Bures J (1997) Retrieval of overtrained place navigation during occlusion of one eye and ipsi- or contralateral blockade of relevant brain centers in rats. Neurobiol Learn Mem 68:60-67.

Fisher RS, Alger BE (1984) Electrophysiological mechansisms of kainic acid-induced epileptiform activity in the rat hippocampal slice. J Neuroscience 4:1312-1323.

Freund TF, Antal M (1988) GABA-containing neurons in the septum control inhibitory interneurons in the hippocampus. Nature 336(6195): 170-173.

Freund TF, Gulyás A, Acsády L, Görcs T, Tóth K (1990) Serotonergic control of the hippocampus via local inhibitory interneurons. Proc Natl Acad Sci USA 87:8501-8505.

Freund TF, Buzsaki G (1996) Interneurons of the hippocampus. Hippocampus 6:347-470.

Gaiarsa JL, Beaudoin M, Ben-Ari Y (1992) Effect of neonatal degranulation on the morphological development of rat CA3 pyramidal neurons: inductive role of mossy fibers on the formation of thorny excrescences. J Comp Neurol 321(4): 612-625.

Gaiarsa JL, Zagrean L, Ben-Ari Y (1994) Neonatal irradiation prevents the formation of hippocampal mossy fibers and the epileptic action of kainate on rat CA3 pyramidal neurons. J Neurophysiol 71:204-215.

Goldschmidt RB, Stewart O (1980) Preferential neurotoxicity of colchicine for granule cells of the dentate gyrus of the adult rat. Proc Natl Acad Sci USA 77:3047-3051.

Gulyás AI, Miettinen R, Jacobowitz DM, Freund TF (1992) Calretinin is present in nonpyramidal cells of the rat hippocampus. I. A new type of neuron specifically associated with the mossy fiber system. Neuroscience 48:1-27.

Gulyás AI, Miles R, Sik A, Tóth K, Tamamaki N, Freund TF (1993) Hippocampal pyramidal cells excite inhibitory neurons through single release site. Nature 366:683-587.

Halasy K, Somogyi P (1993) Subdivisions in the multiple GABAergic innervation of granule cells in the dentate gyrus of the rat hippocampus. Eur J Neurosci 5:411-429.

Hestrin S, Nicoll RA, Perkel DJ, Sah P (1990) Analysis of excitatory synaptic action in pyramidal cells using whole-cell recording from rat hippocampal slices. J Physiol 422:203-225.

Hicks SP, D'Amato CJ (1966) Effects of ionizing radiations on mammalian development. In:. Advances in Teratology (Woollam DHM, ed), pp 195-250. London: Logos Press.

Horváth Z, Czéh G, Czéh B, Seress L (1995) Absence of granule cells does not prevent kainic acid induced pyramidal cell death in the CA3 area of the adult rat hippocampus. Society for Neuroscience Abstracts 21:984.

Hyman BT, van Hoesen GW, Damasio AR, Barnes CL (1982) Alzheimer's disease: Cell-specific pathology isolates the hippocampal formation. Science 225:1168-1170.

Ivanova SF, Bures J (1990) Acquisition of conditioned taste aversion in rats is prevented by tetrodotoxin blockade of a small midbrain region centered around the parabrachial nuclei. Physiol Behav 48(4): 543-549.

Jacobowitz DM, Winsky L (1991) Immunocytochemical localization of calretinin in the forebrain of the rat. J Comp Neurol 304:198-218.

Jarrard LE (1973) The hippocampus and motivation. Psychol Bull 79:1-12.

Jarrard LE (1983) Selective hippocampal lesions and behavior: effects of kainic acid lesions on performance of place and cue tasks. Behav Neurosci 97:873-889.

Jarrard LE (1993) On the role of the hippocampus in learning and memory in the rat. Behav Neural Biol 60: 9-26.

Johansson O, Hökfelt T, Elde RP (1984) Immunohistochemical distribution of somatostatin-like immunoreactivity in the central nervous system of the adult rat. Neuroscience 13:265-339.

Jonas P, Major G, Sakmann B (1993) Quantal components of unitary EPSPs at the mossy fibre synapse on CA3 pyramidal cells of rat hippocampus. J Physiol 472:615-663.

Kolb B, Sutherland RJ, Whisaw IQ (1983) Neonatal hemidecortication or frontal cortex ablation produces similar behavioral sparing but opposite effects on morphogenesis of remaining cortex. Behav Neuroscience 97(1): 154-8.

Kolb B, Walkey J (1987) Behavioural and anatomical studies of the posterior parietal cortex in the rat. Behav Brain Res 23(2): 127-45.

Kotti T, Halonen T, Sirvio J, Riekkinen P Sr, Miettinen R (1997) Comparison of NADPH diaphorase histochemistry, somatostatin immunohistochemistry, and silver impregnation in detecting structural and functional impairment in experimental status epilepticus. Neuroscience 80(1): 105-17.

Kosaka T, Katsumaru H, Hama K, Wu JY, Heizmann CW (1987) GABAergic neurons containing the $Ca^{2+}$-binding protein parvalbumin in the rat hippocampus and dentate gyrus. Brain Res 419(1-2): 119-30.

Köhler C, Chan-Palay V (1982) Somatostatin-like immunoreactive neurons in the hippocampus: an immunohistochemical study in the rat. Neurosci Lett 34:259-264.

Kuno M (1971) Quantum aspects of central and ganglionic synaptic transmission in vertebrates. Physiol Rev 51:647-678.

Lomo T (1971) Patterns of activation in a monosynaptic cortical pathway: the perforant path input to the dentate area of the hippocampal formation. Exp Brain Res 12: 18-45.

Lorente de Nó R (1934) Studies on the structure of the cerebral cortex - II. Continuation of the study of the ammonic system. J Psychol Neurol 46:113-177.

McNaughton BL, Barnes CA, Meltzer J, Sutherland RJ (1989) Hippocampal granule cells are necessary for normal spatial learning but not for spatially-selective pyramidal cell discharge. Exp Brain Res 76: 485-496.

Megias M, Verduga R, Fernandez-Viadero C, Crespo D (1997) Neurons co-localizing calretinin immunoreactivity and reduced nicotinamide

adenine dinucleotide phosphate diaphorase (NADPH-d) activity in the hippocampus and dentate gyrus of the rat. Brain Res 744(1): 112-120.

Mickley GA, Ferguson JL (1989) Enhanced acoustic startle responding in rats with radiation-induced hippocampal granule cell hypoplasia. Exp Brain Res 75:28-34.

Mickley GA, Ferguson JL, Nemeth TJ, Mulvihill MA, Alderks CE (1989) Spontaneous perseverative turning in rats with radiation-induced hippocampal damage. Behav Neurosci 103(4): 722-30.

Mickley GA, Ferguson L, Nemeth TJ (1992) Serial injections of MK 801 (Dizocilpine) in neonatal rats reduce behavioral deficits associated with X-ray-induced hippocampal granule cell hypoplasia. Pharmacology Biochemistry and Behaviour 43:785-793.

Miettinen R, Gulyás AI, Baimbridge KG, Jacobowitz DM, Freund TF (1992) Calretinin is present in nonpyramidal cells of the rat hippocampus. II. Coexistence with other calcium binding proteins and GABA. Neuroscience 48:29-43.

Miettinen R, Sirvio J, Riekkinen P Sr, LaaksoMP, Riekkinen M, Riekkinen P Jr (1993) Neocortical, hippocampal and septal parvalbumin- and somatostatin-containing neurons in young and aged rats: correlation with passive avoidance and water maze performance. Neuroscience 53(2): 367-378.

Moghaddam M, Bures J (1996) Contribution of egocentric spatial memory to place navigation of rats in the Morris water maze. Behav Brain Res 78(2): 121-9.

Mody I, Otis TS, Bragin A, Hsu M, Buzsaki G (1995) GABAergic inhibition of granule cells and hilar neuronal synchrony following ischemia-induced hilar neuronal loss. Neuroscience 69(1): 139-150.

Morris RGM (1981) Spatial location does not require the presence of local cues. Learn Motiv 12:239-260.

Morris RGM, Garrud P, Rawlins JNP, O'Keefe (1982) Place navigation impaired in rats with hippocampal lesions. Nature 297:681-683.

Morris R (1984) Developments of a water-maze procedure for studying spatial learning in the rat. J Neurosci Meth 11:47-60.

Moser E, Moser MB, Andersen P (1993) Spatial learning impairment parallels the magnitude of dorsal hippocampal lesions, but is hardly present following ventral lesions. J Neurosci 13:3916-1925.

Muller RU, Kubie JL, Ranck JB Jr. (1987) Spatial firing patterns of hippocampal complex-spike cells in a fixed environment. J Neurosci 7(7): 1935-1950.

Nadel L (1968) Dorsal and ventral hippocampal lesions and behavior. Physiol Behav 3:891-900.

Nadel L (1991) The hippocampus and space revisited. Hippocampus 1:221-229.

Nadler JV, Perry BW, Cotman CW (1978) Intraventricular kainic acid preferentially destroys hippocampal pyramidal cells. Nature 271:676-677.

Nicoll RA, Malenka RC, Kauer JA (1990) Functional comparison of neurotransmitter receptor subtypes in mammalian central nervous system. Physiol Rev 70:513-566.

Nomura T, Fukuda T, Aika Y, Heizmann CW, Emson-PC, Kobayashi T, Kosaka T (1997) Distribution of nonprincipal neurons in the rat hippocampus, with special reference to their dorsoventral difference. Brain Res 751(1): 64-80.

Obata-Tsuto HL (1987) Light and electron microscopic study of somatostatin-like immunoreactive neurons in the rat hippocampus. Brain Res Bull 18:613-620.

Okazaki MM, Aitken PG, Nadler JV (1988) Mossy fiber lesion reduces the probability that kainic acid will provoke CA3 hippocampal pyramidal cell bursting. Brain Res 440:352-356.

Okazaki MM, Nadler JV (1988) Protective effects of mossy fiber lesions against kainic acid-induced seizures and neuronal degeneration. Neuroscience 26:763-781.

O'Keefe J (1976) Place units in the hippocampus of the freely moving rat. Expl Neurol 51:78-109.

O'Keefe J, Nadel L (1978) The Hippocampus as a Cognitive Map. Clarendon Press, Oxford.

O'Keefe J and Dostrovsky J (1971) The hippocampus as a spatial map. Preliminary evidence from unit activity in the freely-moving rat. Brain Res 34:171-175.

Olton DS, Becker JT, Handelman GE (1979) Hippocampus, sapce and memory. Behav Brain Sci 2:313-365.

Olton DS, Walker JA, Wolf WA (1982) A disconnection analysis of hippocampal function. Brain Res 233:241-253.

Papez JW (1937) A proposed mechanism of emotion. Arch Neurol Psychiatr 38:725-743.

Paxinos G, Watson C (1982) The rat brain in stereotaxic coordinates. Academic Press.

Pulsinelli WA, Brierley JB, Plum F (1982) Temporal profile of neuronal damage in a model of transient forebrain ischemia. Ann Neurol 11(5): 491-498.

Ramón y Cajal S (1893) Estructura del asta de Ammon y fascia dentata. Ann Soc Esp Hist Nat 22:53-114.

Redman S (1990) Quantal analysis of synaptic potentials in neurons of the central nervous system. Physiol Rev 70:165-198.

Represa A, Dessi F, Beaudoin M, Ben-Ari Y (1991) Effects of neonatal gamma-ray irradiation on rat hippocampus-I. Postnatal maturation of hippocampal cells. Neuroscience 42(1): 137-50.

Ribak CE, Navetta MS (1994) An immature mossy fiber innervation of hilar neurons may explain their resitance to kainate-induced cell death in 15-day-old rats. Dev Brain Res 79:47-62.

Rosene DL, Van Hoesen GW (1987) The hippocampal formation of the primate brain. In: Cerebral Cortex 4. Eds: A Peters and EG Jones. Plenum Press: New York.

Save E, Buhot MC, Foreman N, Thinus-Blanc C (1992) Exploratory activity and response to a spatial change in rats with hippocampal or posterior parietal cortical lesions. Behav Brain Res 47(2): 113-27.

SaveE, Moghddam M (1996) Effects of lesions of the associative parietal cortex on the acquisition and use of spatial memory in egocentric and allocentric navigation tasks in the rat. Behav Neurosci 110(1): 74-85.

Scharfman HE (1992) Differentiation of rat dentate neurons by morphology and electrophysiology in hippocampal slices: granule cells, spiny hilar cells and aspiny 'fast-spiking' cells. Epilepsy Res Suppl 7: 93-109.

Schiller J, Schiller Y, Clapham DE (1998) NMDA receptors amplyfy calcium influx into dendritic spines during associative pre- and postsynaptic activation. Nature Neurosciense 1:114-118.

Schuster G, Cassel JC, Will B (1997) Comparasion of the behavioral and morphological effects of colhicine- or neutral fluid-induced destruction of granule cells in the dentate gyrus of the rat. Brief Report, Neurobiol Learn Mem 68: 86-91.

Seress L (1988) Interspecies comparison of the hippocampal formation shows increased emphasis on the regio superior in the Ammon's horn of the human brain J Brain Res (J Hirnforschung) 29: 335-340.

Scoville WB, Milner B (1957) Loss of recent memory after bilateral hippocampal lesions. J Neurol Neurosurg Psychiatr 20:11-21.

Schmidt-Kastner R, Freund TF (1991) Selective vulnerability of the hippocampus in brain ischemia. Neuroscience 40(3): 599-636.

Sloviter RS, Nilaver G (1987) Immunocytochemical localization of GABA-, cholecystokinin-, vasoactive intestinal polypeptide-, and somatostatin-like immunoreactivity in the area dentata and hippocampus of the rat. J Com Neurol 256:24-60.

Sloviter RS, Valiquette G, Abrams GM, Ronk EC, Sollas AL, Paul LA, Neuborts S (1989) Selective loss of hippocampal granule cells in the mature rat brain after adrenalectomy. Science 243:535-538.

Sloviter RS (1992) Possible functional consequences of synaptic reorganization in the dentate gyrus of kainate-treated rats. Neurosci Lett 137:91-96.

Sloviter RS, Sollas AL, dean E, Neuborts S (1993) Adrenalectomy-induced granule cell degeneration in the rat hippocampal dentate gyrus; characterization of an *in vivo* model of controlled neuronal death. J Comp Neurol 330:324-336.

Sperber EF, Haas KZ, Stanton PK, Moshe SL (1991) Resistance of immature hippocampus to seizure-induced synaptic reorganization. Dev Brain Res 60:88-93.

Squire LR (1987) Memory and Brain. Oxford University Press, New York.

Stanfield BB, Cowan WM (1988) The development of the hippocampal region. In: A Peters, EG Jones (Eds.) Cerebral Cortex 7, Development and Maturation of Cerebral Cortex, Plenum Press, New York, pp. 91-130.

Steward O, Scoville SA (1976) Cells of origin of entorhinal cortical afferents to the hippocampus and fascia dentata in the rat. J Comp Neurol 169:347-370.

Stewart-Amidei C (1995) Delayed effects of therapeutic brain irradiation. Crit Care Nurs Clin North Am 7(1): 125-33.

Stricker C, Field AC, Redman SJ (1996) Statistical analysis of amplitude fluctuations in EPSPs evoked in rat CA1 pyramidal neurones in vitro. J Physiol 490:419-441.

Stubley-Weatherly L, Harding JW, Wright JW (1996) Effects of discrete kainic acid-induced hippocampal lesions on spatial and contextual learning and memory in rats. Brain Res 716(1-2): 29-38.

Sutherland RJ, Whishaw IQ and Kolb B (1982) Spatial mapping: definitive disruption by hippocampal or medial frontal cortical damage in the rat. Neurosci Lett 31:271-276.

Sutherland RJ, Whishaw IQ and Kolb B (1983) A behavioral analysis of spatial localization following electrolytic, kainate- or colchicine-induced damage to the hippocampal formation in the rat. Behav Brain Res 7:133-153

Tamamaki N, Watanabe K, Nojyo Y (1984) A whole image of the hippocampal pyramidal neuron revealed by intracellular pressure-injection of horseradish peroxidase. Brain Res 307:336-340.

Tauck DL, Nadler JV (1985) Evidence of functional mossy fiber sprouting in hippocampal formation of kainic acid-treated rats. J Neurosci 5:1016-1022.

Timm F (1958) Zur Histochemie des Ammonhorngebietes. Z Zellforsch Microsc Anat 48:548-555.

Thomson AM, West DC, Deuchars J (1995) Properties of single axon excitatory postsynaptic potentials elicited in spiny interneurons by action potentials in pyramidal neurons in slices of rat neocortex. Neuroscience 69:727-738.

Tóth K, Freund TF, Miles R (1997) Disinhibion of rat hippocampal pyramidal cells by GABAergic afferents from the septum. J Physiol 500:463-474.

Valtshanoff JG, Weinberg RJ, Kharazia VN, Nakane M and Schmidt H (1993) Neurons in rat hippocampus that synthesize nitric oxide. J Comp Neurol 331: 111-121.

Vida I, Halasy K, Szinyei C, Somogyi P, Buhl EH (1998) Unitary IPSPs evoked by interneurons at the stratum radiatum - stratum lacunosum-moleculare border in the CA1 area of the rat hippocampus in vitro. J Physiol 506:755-773.

Vincent RS, Kimura H (1992) Histochemical mapping of nitric oxide synthase in the rat brain. Neuroscience 46:755-784.

Volpe BT, Hirst W (1983) The characterization of an amnesic syndrome following hypoxic ischemic injury. Arch Neurol 40:436-440.

Volpe BT, Davis HP, Towle A, Dunlap WP (1992) Loss of hippocampal CA1 pyramidal neurons correlates with memory impairment in rats with ischemic or neurotoxin lesions. Behav Neurosci 106(3): 457-64.

Westbrook GL, Lothman EW (1983) Cellular and synaptic basis of kainic acid-induced hippocampal epileptiform activity. Brain Res 273:97-109.

Wilson MA, McNaughton BL (1993) Dynamics of the hippocampal ensemble code for space. Science 261:1055-1058.

Witter MP, Griffioen AW, Jorritsma-Byham B, Krijnen JLM (1988) Entorhinal projections to the hippocampal CA1 region in the rat: an underestimated pathway. Neurosci Lett 85, 193-198.

Whishaw IQ (1987) Hippocampal, granule cell and CA3-4 lesions impair formation of a place learning-set in the rat and induce reflex epilepsy Behav Brain Res 24 59-72.

Wolf G, Keilhoff G (1984) Kainate and glutamate neurotoxicity in dependence on the postnatal development with special reference to hippocampal neurons. Dev Brain Res 14:15-21.

Wood ER, Mumby DG, Pinel JP, Phillips AG (1993) Impaired object recognition memory in rats following ischemia-induced damage to the hippocampus. Behav Neurosci 107(1): 51-62.

Yeckel MF, Barrionuevo G, Berger TW (1988) In vivo electrophysiological evidence for monosynaptic input from the entorhinal cortex to pyramidal cell regions of the hippocampus. Soc Neurosci Abstr 14: 246.

Zhuravin IA, Bures J (1991) Extent of the tetrodotoxin induced blockade examined by pupillary paralysis elicited by intracerebral injection of the drug. Exp Brain Res 83(3):687-90.

Zola-Morgan S, Squire LR, Amaral DG (1986) Human amnesia and the medial temporal region: enduring memory impairment following a bilateral lesion limited to field CA1 of the hippocampus. J Neurosci 6(10): 2950-67.

## Chapter 9.

# PUBLICATION LIST OF THE AUTHOR

## Scientific papers:

1. Czurkó A, **Czéh B**, Seress L, Nadel L, Bures J: Severe spatial navigation deficit in the Morris water maze after single high dose of neonatal X-ray irradiation in the rat. *Proc Natl Acad Sci USA*, 94: 2766-2771.
2. **Czéh B**, Seress L, Czéh G: Residual granule cells can maintain susceptibility of CA3 pyramidal cells to kainate induced epileptiform discharges. *Hippocampus* (in press)
3. **Czéh B**, Seress L, Nadel L, Bures J: Lateralized fascia dentata lesion and blockade of one hippocampus: effect on spatial memory in rats. Rapid Communication, *Hippocampus* (in press)
4. **Czéh B**, Seress L, Czéh G: Electrophysiological characteristics and morphological properties of dentate granule- and CA3 pyramidal cells in slices cut from neonatally irradiated rats.
   submitted manuscript to *Neurobiology*
5. **Czéh B**, Seress L: The numerical distribution and co-localization of the nicotinamide adenine dinucleotide phosphate diaphorase (NADPH-d) reactive cells in the hippocampus and dentate gyrus of the rat. *manuscript*

## Abstracts of posters at Congresses:

1. Horváth Z, Czéh G, **Czéh B**, Seress L: Absence of granule cells does not prevent kainic acid induced pyramidal cell death in the CA3 area of the adult rat hippocampus. *Society for Neuroscience Abstracts*, 21. San Diego, 1995.

2. **Czéh B**, Czurkó A, Seress L: Distribution of NADPH-d positive cells in the hippocampus following neonatal X-ray irradiation induced granule cell loss. ENA/EBBS Meeting, *European Journal of Neuroscience Suppl.* no 8. p:14, 1995

3. Czéh G, **Czéh B**: Functional and morphological characterization of CA3 principal cells of the neonatally irradiated rat hippocampus. ENA/EBBS Meeting, Berlin, *European Journal of Neuroscience Suppl.* no. 10. p:389, 1996

4. Czurkó A, **Czéh B**, Seress L: Number and distribution of interneurons in the hippocampus of the rat and monkey. 3rd Congress of Hungarian Neuroscience Association, Balatonfüred, Hungary, *Neurobiology,* 4 (3), 1996

5. **Czéh B**, Czéh G, Seress L: Kainic acid evokes epileptiform discharges in the CA3 area of slice preparations from X-ray irradiated rats. 3rd Congress of Hungarian Neuroscience Association, Balatonfüred, Hungary, *Neurobiology,* 4 (3), 1996

6. **Czéh B,** Czurkó A, Seress L, Nadel L, Bures J: Granule cell loss of the dentate gyrus impairs spatial learning in the X-ray irradiated rats. ENA/EBBS Meeting, Strasbourg, *European Journal of Neuroscience Suppl.* no. 9. p:173, 1996

7. **Czéh B**, Seress L, Houser C: Number and distribution of $GAD_{65}$ mRNA-containing neurons in the rat hippocampal formation. 4th Congress of Hungarian Neuroscience Association, Gödöllô, Hungary, *Neurobiology,* 5 (1), 1997

8. **Czéh B**, Seress L, Nadel L, Bures J: Lateralized fascia dentata (FD) lesion and blockade of one hippocampus: Effect on spatial memory in rats. ENA/EBBS Meeting, Berlin, *European Journal of Neuroscience Suppl.* no. 10. p:366, 1998

9. **Czéh B**, Pokorny J, Seress L, Nadel L, Bures J: Morphological correlates of the spatial navigation deficit induced by single high dose of neonatal X-ray irradiation in the rats. The 6th Neuropharmacology

Conference, Cortical Plasticity, The Representation of Experience. An Official Satellite of ENA/EBBS Meeting, Berlin, 1998

## Abstracts of oral presentations at Congresses:

10. Seress L, **Czéh B**, Horváth Z: Regeneration and plasticity in the X-irradiated hippocampus 2nd Congress of Hungarian Neuroscience Association, Szeged, Hungary, *Neurobiology,* 3 (1), 1995
11. Czéh G, **Czéh B**: An intracellular study of kainic acid induced hyperexcitability of CA3 pyramidal cells. 4th Congress of Hungarian Neuroscience Association, Gödöllô, Hungary, *Neurobiology,* 5 (1), 1997
12. **Czéh B,** Seress L, Czéh G: Functional and morphological characterization of CA3 pyramidal cells of the neonatally irradiated rat hippocampus. 5th Congress of Hungarian Neuroscience Association, Debrecen, Hungary, *Neurobiology*, (in press), 1998